NATIONAL BUREAU OF STANDARDS REPORT

5704

FLEXURAL TESTS OF BEAMS WITH REINFORCEMENT OF DIFFERENT PROPERTIES

by

Robert G. Mathey and D. Watstein

Report to

American Iron and Steel Institute

U. S. DEPARTMENT OF COMMERCE
NATIONAL BUREAU OF STANDARDS

THE NATIONAL BUREAU OF STANDARDS

Functions and Activities

The functions of the National Bureau of Standards are set forth in the Act of Congress, March 3, 1901, as amended by Congress in Public Law 619, 1950. These include the development and maintenance of the national standards of measurement and the provision of means and methods for making measurements consistent with these standards; the determination of physical constants and properties of materials; the development of methods and instruments for testing materials, devices, and structures; advisory services to Government Agencies on scientific and technical problems; invention and development of devices to serve special needs of the Government; and the development of standard practices, codes, and specifications. The work includes basic and applied research, development, engineering, instrumentation, testing, evaluation, calibration services, and various consultation and information services. A major portion of the Bureau's work is performed for other Government Agencies, particularly the Department of Defense and the Atomic Energy Commission. The scope of activities is suggested by the listing of divisions and sections on the inside of the back cover.

Reports and Publications

The results of the Bureau's work take the form of either actual equipment and devices or published papers and reports. Reports are issued to the sponsoring agency of a particular project or program. Published papers appear either in the Bureau's own series of publications or in the journals of professional and scientific societies. The Bureau itself publishes three monthly periodicals, available from the Government Printing Office: The Journal of Research, which presents complete papers reporting technical investigations; the Technical News Bulletin, which presents summary and preliminary reports on work in progress; and Basic Radio Propagation Predictions, which provides data for determining the best frequencies to use for radio communications throughout the world. There are also five series of nonperiodical publications: The Applied Mathematics Series, Circulars, Handbooks, Building Materials and Structures Reports, and Miscellaneous Publications.

Information on the Bureau's publications can be found in NBS Circular 460, Publications of the National Bureau of Standards ($1.25) and its Supplement ($0.75), available from the Superintendent of Documents, Government Printing Office, Washington 25, D. C.

Inquiries regarding the Bureau's reports should be addressed to the Office of Technical Information, National Bureau of Standards, Washington 25, D. C.

NATIONAL BUREAU OF STANDARDS REPORT

NBS PROJECT		NBS REPORT
1001-12-4814	December 30, 1957	5704

FLEXURAL TESTS OF BEAMS WITH REINFORCEMENT OF DIFFERENT PROPERTIES

by

Robert G. Mathey and D. Watstein

To

American Iron and Steel Institute

U. S. DEPARTMENT OF COMMERCE

NATIONAL BUREAU OF STANDARDS

Contents

Tables

Figures

FLEXURAL TESTS OF BEAMS WITH REINFORCEMENT OF DIFFERENT PROPERTIES

by

Robert G. Mathey and D. Watstein

Abstract

The effect of magnitude of steel stresses on the center deflection, strain in the concrete, widths and spacing of cracks in the region of constant bending moment, maximum load carrying capacity, and the manner of failure was investigated in a series of flexural beam tests. This series consisted of 12 beams having a cross section of 6- by 15-in. and a span of 10 ft with the load applied at the quarter points.

Six types of deformed bars with yield strengths ranging from 40,000 to 100,000 psi and different stress-strain characteristics were used as tensile reinforcement. The ratio of reinforcement in the beams was proportioned inversely to the yield strength, thus providing equal resistance to yielding under tensile forces. Failure occurred in all of the beams at approximately the same load. The relationship between the computed steel stresses and the center deflections, width and spacing of cracks, and strain in the steel and concrete was determined for the six types of steel.

1. INTRODUCTION

The current interest in the properties of reinforced concrete beams containing high-strength deformed steel bars has prompted the National Bureau of Standards to undertake a study of the effect of magnitude of steel stresses on the behavior of flexural members. This study is being supported at the National Bureau of Standards by a grant made by the Committee on Reinforced Concrete Research of American Iron and Steel Institute. The present

report representing a completed initial phase of this study deals with the effect of steel stresses on the flexural rigidity, width and spacing of cracks and the strains in the concrete and steel.

Tests described in this report were carried out with beams reinforced with six types of deformed bars which differed both in their yield strengths and in their stress-strain characteristics. The yield strengths ranged from 40,000 to 100,000 psi; some of the steels had well defined yield strengths while others exhibited gradual yielding. The modulus of elasticity of one of the bars was significantly lower than that of the other five types of bars.

The beams were all of the same size, and concrete of the same quality was used for all beams. The ratio of longitudinal reinforcement was proportioned inversely to the yield strength so that the total resistance to yielding of the tensile reinforcement was practically constant in all specimens. The beams were designed to fail in tension, and bond and shear failures were precluded by the use of adequate shear reinforcement and anchorage. Observations were taken under load to determine deflections, strain in the steel and concrete, widths and spacing of cracks in the region of uniform bending moment, and the maximum load which was sustained.

2. DESCRIPTION OF MATERIALS AND TEST SPECIMENS

2.1 Beam specimens

The specimens were reinforced concrete beams having a cross section of 6- by 15-in. and an effective depth of 12.8 in. The beams were 13 ft long and were tested over a span of 10 ft. The arrangement of the reinforcing bars, dimensions of the beams and the method of loading are illustrated in figure 1. The specimens were loaded at the quarter points and tested as simply supported beams.

The test beams are described in Table 1. The first symbol (F) in the beam designation signifies a flexural beam specimen. The second symbol (Roman numeral from I to VI) designates the type of steel bar; the letter A following I and V indicates that the original steel shipment was found to be unsuitable and a second lot of steel was procured in these two cases. The last number in the designation denotes the serial number of the beam specimen.

The ratio of longitudinal reinforcement ranged from a maximum of 2.55 percent for steel IA having a nominal yield strength of 40,000 psi, to a minimum of 1.12 percent for steel having a yield strength of 100,000 psi. The actual total force causing yielding of the tensile reinforcement, $f_y A_s$, as determined by tests of coupons of the reinforcing bars ranged from 81,600 to 90,300 lb.

Stirrups placed in the shear portion of the beam span and tied to the longitudinal reinforcement were used to safeguard against diagonal tension failures. Steel plates, 4- by 6- by 1/4 in. were welded to the ends of the tensile reinforcement to prevent bond failures.

2.2 Reinforcement

Six types of deformed bars with various stress strain characteristics were used for longitudinal reinforcement. The nominal yield strengths of these steels were 40,000 psi for Type IA, 65,000 psi for Types II, III, and IV, and 100,000 psi for Types VA and VI. A tensile coupon from each bar size was tested to rupture. Tensile properties of the bars are listed in Table 2, and a typical stress-strain curve for each bar is given in figure 2. The yield strengths of the steels varied from +8.5 percent for Type IV steel to -1.2 percent for Type VA steel from the specified or nominal values. Types IA and II steels exhibited a well defined yield strength, and that was determined by "halt of the gage method." Steels III, IV, VA, and VI, exhibited gradual yielding and their yield strengths were determined by the "0.2 percent offset method." Type VA steel was specified to have a well defined yield strength, but did not fully meet this requirement. While steel VA did not exhibit a sharply defined yield strength, its stress-strain characteristic was essentially linear up to a stress well above 80,000 psi. Nevertheless, its yield strength was determined by the "offset" method in order to avoid ambiguity.

All of the bars were conventional round reinforcing bars with diamond shaped deformations except the bars of Type IV steel. The Type IV bar was a cold twisted, ribbed bar with a dumbbell shaped cross section (Fig. 3). Height, width, spacing, and projected length of the deformations were measured on one coupon from each bar size. The properties of deformations appear in Tables 2 and 3. Deformations of all the reinforcing bars met the requirements of ASTM A305-53T.

2.3 Concrete

The concrete was made from a mix of Type I cement, sand, and gravel proportioned approximately 1:3.2:4.1 by weight. The sand and gravel were silicious aggregates from White Marsh, Maryland. The maximum size of the coarse aggregate was 1 in. and the fineness modulus of the sand was 2.71. Grading of these aggregates is given in Table 4. Water content of the concrete was about 7.7 gal per sack and the slump ranged from 3 to 6 in. The average compressive strength obtained from tests of control cylinders was 3650 psi; values for individual specimens tested for each beam are given in Table 1.

2.4 Fabrication and curing

The stirrups and ties were fabricated in the laboratory and the reinforcement was assembled into a unit before it was placed in the forms. The deformations were filed off for a length of about 3/4 in. on each side of the bars at the center of span to facilitate the placement of bonded wire electric strain gages. Two gages were placed on each longitudinal reinforcing bar and the gages and lead wires were waterproofed with Petrosene wax.

Specimens were cast in steel forms with the tensile reinforcement near the bottom. After five days they were removed from the forms and moist-cured until two days prior to testing at 28 to 30 days. One control cylinder was cast from each of the three batches that were used to cast a beam specimen. The three standard 6- by 12-in. cylinders were stored and cured in the same manner as the specimen. The cylinders were tested at the same age as the specimen to determine the compressive strength and the modulus of elasticity of the concrete. All concrete was mixed in a tilting drum type mixer of 7 cu ft capacity and placed with the aid of a laboratory type internal vibrator.

3. TESTING PROCEDURE

3.1 Test setup

The specimens were tested as simply supported beams over a span of 10 ft in a 600,000 lb capacity hydraulic machine. To facilitate the placement and reading of Tuckerman optical strain gages on the tension face of the beam, the beams were placed in the testing machine in an inverted position. A sketch of the method of loading and location of Tuckerman

strain gages is shown in figure 4. Rockers were used to support the beams at the quarter points and the load was applied through a steel loading beam with knife edges attached at each end. The forces were distributed at the load and reaction points through steel bearing plates 3 1/2 in. wide that covered the entire width of the specimen. The bearing plates at the reaction points were 1 in. thick. The bearing plate was 1 1/2 in. thick under one of the knife edges and under the other, three 1/2 in. steel rollers rested on a 1-in. bearing plate. A photograph of a beam in the testing machine prior to testing is shown in figure 5.

3.2 Instrumentation

The widths of cracks were measured with 11 Tuckerman optical strain gages arranged in two rows located at equal distances from the longitudinal center line of the specimen. The gages in the two rows were staggered and overlapped 0.5 in. to include every crack which formed in the region of constant bending moment. (Location of the Tuckerman strain gages on the specimen is shown in figure 4). The Tuckerman gages had a gage length of 6 in. and a 0.5 in. lozenge. The gages were placed on brass bearing strips attached to the surface of the concrete with epoxy resin cement. The gages were held firmly in place with rubber bands attached to brass anchorage disks cemented to the concrete in a similar manner. These gages were equipped with 45 degree prisms to enable observations to be made with the auto-collimator in a horizontal position.

The Tuckerman gage readings after formation of a crack were taken to represent the width of crack spanned by the given gage and no attempt was made to correct the crack width for the tensile strains observed in the concrete prior to formation of cracks within the gage length. In some of the test specimens two or three cracks occurred in the same gage length while no cracks would occur in another gage length. Compressive strains were observed in a few cases on the tensile face of the beam where there were no cracks through the gage length, while the adjoining gages spanned cracks. The compressive strain continued to increase with the tensile stress in the reinforcement as long as no additional cracks formed between the original pair of adjacent cracks. This phenomenon was also observed by Clark [1] * and investigated more fully by use of tensile bond specimens [2] .

* Figures in brackets indicate literature references at the end of the paper.

The average spacing of cracks was determined from the number of cracks and the distance between the two outermost cracks that occurred within the region of constant bending moment.

Deflections at the center of span and 2 ft from the center were measured with 0.001-in. dial gages attached to aluminum bars whose ends were supported at the sides of the beams under the loading points. The gages were located as shown in figure 1. The gages bore on angle clips attached to the concrete by screws. The aluminum bars with the attached dial gages were removed prior to failure. Deflections were then measured at the center of span by scales attached to the specimen and a taut wire stretched between two points on the side of the beam directly under the loading points.

Strains in the tensile reinforcement were measured with bonded wire electrical resistance strain gages attached diametrically opposite at mid plane of the longitudinal bars. The gages were of type AB-7, with a gage length of 1/4 in. and were located at mid span. The gages were attached with epoxy resin cement and waterproofed with Petrosene wax.

The compressive strains in the concrete were also measured with bonded wire electric resistance strain gages. These gages were of type A-1, with a gage length of 13/16 in. They were located at the center and at positions of 2 ft on either side of the center of span along the longitudinal center line of the specimen on the compressive face of concrete. These gages were located as shown in figure 1. The gages were attached to the concrete with epoxy resin cement.

3.3 Test procedure

The loading beam was placed in position, as shown in figure 5, and the gages were read at zero machine load. A load of 1000 lb was applied and released and the gages were again read at zero machine load. The load was then applied in increments of 2500 lb up to a load of 15,000 lb and then in increments of 5000 lb to failure. Each increment of the load was applied at a rate of 4000 lb per min. The following measurements were recorded after each increment of applied load: deflections along beam, the strains in the reinforcement, the strains in the concrete, the width of cracks in the region of constant bending moment, and the applied load at which the measurements were observed. In addition to these measurements the location and extent of cracks were recorded immediately after the application of each increment.

The loading beam was placed in position before attaching the Tuckerman strain gages to the beam specimen. This procedure was followed to prevent any damage to the Tuckerman gages. The steel loading beam weighed 1300 lb and the beam specimen weighed 1400 lb. At zero machine load, the summation of moments at the center of span was equal to 2150 ft-lb, corresponding to an effective initial load of 1.72 kips. In the computations a correction factor of 1.72 kips was added to the machine load.

Observed strains in the steel and concrete were very small for the first increment of the applied load; therefore, no attempt was made to correct the strain measurements for the initial load. However, the deflections were corrected for the deflection corresponding to the initial load. The corrections were computed using the formula given on page 11; their values ranged from 0.0096 in. in beams with Type IA steel to 0.0179 in. in beams with Types VA and VI steels.

4. TEST RESULTS

4.1 Mode of failure and load carrying capacity

The control beams were reinforced with Type 1A steel and were designed to fail by yielding of the tensile reinforcement. Tensile failures occurred in all the beams except the beams that were reinforced with steels having nominal yield strengths of 100,000 psi. Beams F-VA-17 and F-VI-18 failed by compression of the concrete while tensile and compressive failures occurred simultaneously in beams F-VA-19 and F-VI-9. The use of adequate shear and bond reinforcement limited the mode of failure in this investigation to tension or compression. Photographs of all the beams after failure occurred are shown in figures 6 and 7.

The maximum load carrying capacity of the beams ranged from 61,700 to 67,500 lb with an average maximum load of 64,000 lb; the deviation of loads at failure from the mean ranged from +5.5 to -3.6 percent. Since all of the beams failed at approximately the same load, the maximum load carrying capacity of the beams was not affected by the type of longitudinal reinforcement whose areas were proportioned to give a constant total yield strength of the tensile reinforcement. The maximum load and mode of failure for the individual beams are given in Table 1.

4.2 Deflections of beams

The relationship between the applied load and the midspan deflection is shown in figure 8. Each curve plotted on this graph represents the average results obtained with two beam specimens. As expected, the deflections increased as the percentage of longitudinal reinforcement was reduced. The deflections of beams reinforced with Type IV steel departed considerably from the deflections of beams reinforced with comparable steels of Type II and Type III. This departure is explained by the fact that the modulus of elasticity of Type IV bars was 12 percent lower than the modulus of Types II and III bars. (See Table 2).

Load vs. midspan deflection curves to the point of failure are shown in figure 9 for individual beam specimens.

The effect of higher steel stress on the deflection is shown more directly in figure 10. This graph presents relative deflection values for loads of 28.5, 42.9, and 57.1 kips which produce respectively theoretical steel stresses of 20,000, 30,000, and 40,000 psi in beams with Type IA steel. Similarly, at a load that produces a steel stress of 20,000 psi in beams with Type IA steel, the computed stress in the steel with a 65,000 psi yield strength will be 32,500 psi and the computed stress in 100,000 psi yield strength steel will be 50,000 psi. For the purpose of direct comparison, the deflections are taken as unity in beams with Type IA reinforcement. For a stress equal to one-half the nominal yield strength of the steel, deflections in beams with 65,000 psi reinforcement ranged from 40 to 53 percent greater than the control beams. The deflections in beams with 100,000 psi reinforcement ranged from 80 to 93 percent greater than in the control beams.

Similar comparisons of the deflections for stresses of 75 and 100 percent of the nominal yield strengths of the steels are also shown in figure 10.

4.3 Stress in reinforcement

The relationship between the applied load and the observed stress in the reinforcement is shown in figure 11. Each curve on this graph is an average of the observed values for two beam specimens. The data for beams reinforced with Type VA steel are omitted because of faulty performance of the strain gages.

The strains in the reinforcement were measured at the center of span. The observed strains were converted into stresses by means of the stress-strain curves shown in figure 2.

Beams reinforced with Types IA, II, III and IV steels failed by yielding of the steel. The maximum observed stresses in steels IA, II, III and IV approached the yield strengths determined in the tensile tests. However, the observed stress in the reinforcement in beams with Type VI steel was 80,000 psi at a load equal to 95.7 percent of the maximum load; the theoretical stress at this load was 94,000 psi.

4.4 Concrete strains

The applied load-compressive strain data are presented graphically in figure 12. Each curve on this graph represents the average results obtained with two beam specimens. The compressive strains were measured on the surface of concrete and the strain gages were located as shown in figure 1. As expected, the compressive strain in the concrete increased as the percentage of longitudinal reinforcement was reduced. The compressive strains in beams with Type IV steel were considerably greater than in beams with comparable steels of Types II and III. This is attributed partly to the lower modulus of elasticity of Type IV bars.

A comparison of compressive strains in beams supporting equal loads is shown in figure 13. The effect of higher steel stresses on the compressive strains is brought out clearly in this graph. At a stress of one-half the nominal yield strength of the reinforcement the compressive strains in beams with 65,000 psi reinforcement range from 5 to 24 percent greater than in the control beams. In beams with 100,000 psi reinforcement, the compressive strains ranged from 25 to 37 percent greater than in the control beams. Similar comparisons of the compressive strains for stresses of 75 and 100 percent of the nominal yield strengths of the steels are also shown in figure 13.

4.5 Widths and spacing of cracks

The relationship between the applied load and the average width of cracks is shown in figure 14. Each curve in this figure represents the results obtained from two beam specimens. The cracks were measured on the tensile surface of the beam in the region of constant bending moment. (See Fig. 1). The

effect of higher steel stresses is brought out particularly clearly in figure 14, where the load-width of crack curves fall into three distinct groups corresponding to the nominal yield strengths of 40,000, 65,000, and 100,000 psi. As expected, the width of cracks increased markedly as the percentage of longitudinal reinforcement was reduced.

The ratio of the average width of cracks in beams reinforced with high yield strength steels to the width of crack in beams with steel of Type IA and supporting equal loads is shown in figure 15. For the purpose of direct comparison the widths of cracks are taken as unity in beams with Type IA steel. For a stress of one half the nominal yield strength of the steel in beams with 65,000 psi reinforcement the average width of cracks ranged from 60 to 76 percent greater than in the control beams. In beams reinforced with 100,000 psi steel, the width of cracks ranged from 164 to 168 percent greater than in the control beams. Similar comparisons of the widths of cracks for steel stresses of 75 and 90 percent of the nominal yield strengths of the steels are also shown in figure 15.

The relationship between the average width of cracks and the computed stress in the reinforcement is shown in figure 16; this figure includes the crack data for all the beams. The slopes of the stress-crack width curves varied within narrow limits and appeared to be independent of the ratio of reinforcement and in case of Type IV steel, of the modulus of the steel. The effect of lower modulus of elasticity in Type IV steel was probably minimized by the somewhat smaller average spacing of cracks in beams containing that steel than the spacing in beams with steels of Types II and III.

The relationship between the theoretical stress in the reinforcement and spacing and width of cracks is shown in figure 17. Each curve represents the average results obtained with two beam specimens. The minimum average spacing of cracks in the control beams was 4.2 in. For beams with 65,000 psi yield strength reinforcement this minimum spacing of cracks ranged from 4.2 to 4.6 in., and for beams with 100,000 psi reinforcement, this minimum spacing ranged from 4.7 to 5.3 in. This is an indication that the minimum average spacing of cracks will increase with a decrease in the percentage of longitudinal reinforcement and higher tensile stresses. The minimum spacings of cracks for the individual beams are given in Table 1.

In view of the consistently greater spacing of cracks observed in beams with reduced ratios of reinforcement, it would be expected that at a given stress in steel the average width of cracks would be somewhat greater in beams containing the lesser amounts of reinforcement. It is believed that the effect of greater spacing of cracks on the width of cracks was offset by the fact that the reduction of steel ratio was achieved by using smaller diameter bars; it is known that the effective modulus of elasticity of embedded deformed bars is materially increased as the diameter of bars is reduced [2] .

5. COMPARISON OF EXPERIMENTAL AND THEORETICAL RESULTS

The comparisons of experimental and theoretical values of the midspan deflections, stress in reinforcement, and the compressive strain in the concrete are shown graphically in figures 18, 19, and 20 respectively. The theoretical values of the variables were determined by the conventional "straight-line" theory. A comparison of the experimental and theoretical results of the average width of cracks is shown in figure 21. The theoretical values for the average width of cracks were determined from an expression developed by Chi and Kirstein [3] , and a brief explanation of this expression is given on page 13.

In computing the theoretical values of the variables the observed values of moduli of elasticity of steel and concrete were utilized. The modulus of elasticity of concrete was the secant value determined for $0.5\ f'_c$, while the modulus of steel was the value corresponding to the linear portion of the stress-strain curve.

The load-deflection curves for beams reinforced with steels of Types IA, II, and III show good agreement between observed and theoretical values (Fig. 18). The theoretical deflections were determined from the expression,

$$\triangle = \frac{11\ M\ L^2}{96\ E_c\ I}$$

where E_c = modulus of elasticity of concrete
I = moment of inertia of beam cross section transformed to concrete = $1/3\ bk^3d^3 + nA_s(1-k)^2d^2$
L = length of beam span
M = bending moment
n = observed modular ratio

The theoretical midspan deflections plotted in figure 18 are terminated at the calculated yield point of the beam as indicated on the graph. The maximum observed load is also shown in each case by a short dash at the extremity of the load-deflection curve.

It was observed that the agreement between the computed and observed deflections was better for steels having a linear stress-strain characteristic than for comparable steels exhibiting gradual yielding. Thus, beams with steel of Type IV showed a greater departure of computed from observed deflections than did beams with steels of Type II and III, while beams with steel of Type VI showed a greater departure than did beams with steel of Type VA. The observed deflections of all the beams were less than the calculated values up to a stress of one-half the nominal yield strength of the reinforcement.

A comparison of the theoretical and observed stress in the steel reinforcement is shown in figure 19. Each curve represents the results obtained from two beam specimens. Steel stress data from beams reinforced with Type VA steel were omitted from this figure because of unreliable strain data. The observed strains were converted into stresses by means of the stress-strain curves shown in figure 2.

The observed and theoretical values of steel stresses show good agreement for beams reinforced with Type IA steel. However, the observed stress in the reinforcement is considerably less than the theoretical stress in beams reinforced with the higher yield strength steels. This is particularly true in beams reinforced with Type VI steel. The use of the "straight line" theory thus yielded calculated stresses that were in excess of observed stresses in all cases; the difference between the observed and computed stresses increased as the diameter of bar decreased.

The theoretical and observed strains in the concrete are compared in figure 20. Each curve represents the results obtained from two beam specimens. The theoretical strain was determined from the calculated compressive stress at the surface of concrete and the observed modulus of elasticity of the concrete. One control cylinder that was cast with each beam specimen was used to determine the stress-strain characteristics of the concrete. The value of the modulus of elasticity, E_c, was determined by the slope of a line passing through the origin of the stress-strain curve and a point on the curve corresponding to one-half the compressive strength of the

cylinder, $0.5\ f'_c$. The values of the observed compressive strains in the concrete in all cases are less than the theoretical values up to the load producing a stress in the reinforcement of one-half the nominal yield strength.

As in the case of load-deflection relationship, the departure of the observed compressive strains from the computed values at high steel stresses was greater for steels IV, VA, and VI, than for steels IA, II, and III. The departure of observed strains from computed values was particularly marked for steels IV and VI whose strain-strain characteristics showed the greatest departure from linearity.

The observed and theoretical values of the average width of cracks are compared in figure 21. Each curve represents the results obtained from two beam specimens.

The paper, "Flexural Cracks in Reinforced Concrete Beams," by Michael Chi and Arthur F. Kirstein has not yet been published. Therefore, a brief explanation of the equation for determining the width of cracks in reinforced concrete flexural beams is given in the following pages.

The average width of crack at the reinforcing steel is given by the equation:

$$W_s = 5\,\phi\,D\,\frac{f_s - \frac{2500}{\phi D}}{E_s} \qquad (1)$$

where

$$\phi = \frac{A_t}{m^2 A_s} \qquad (2)$$

A_s = area of reinforcing steel

A_t = area of concrete effected by the extension of the steel

D = diameter of reinforcing bar

E_s = modulus of elasticity of the steel (linear portion of the stress-strain curve)

f_s = steel stress

m = factor determining the diameter of the concrete area effected by the extension of the reinforcing steel.

ϕ = ratio of the assumed effective area to the fully developed area of concrete

A constant conversion factor was used to convert the average width of crack at the reinforcing steel to the average width of crack at the surface of concrete. The average width of crack at the surface of concrete is given by the equation:

$$W_c = W_s \frac{h-kd}{d-kd} \qquad (3)$$

where d = effective depth of specimen

h = total depth of specimen

kd = depth of compressive concrete in the specimen.

The Chi-Kirstein formula is a semi-empirical expression in which the factors m and $\emptyset$ are derived from the hypothesis that only a portion of the cross section of the beam below the neutral axis resists the tension in the concrete induced by bond stresses. This portion of the tensile cross section is termed "the effective area," and its ratio to the "fully developed area" determines the value of $\emptyset$. These terms are defined in figure 22 in terms of the properties of the cross section of the beam. The values of $\emptyset$ determined for all beam specimens are listed in Table 5. Chi and Kirstein estimated that m = 4 for the Bethlehem bar which they used in their study. It was assumed by the authors that this value of m was also applicable to the deformed steel bars used in this investigation.

In the application of Chi and Kirstein's expression for the average width of cracks, the nominal dimensions of the reinforcing bars were used. For the purpose of computing the coefficient $\emptyset$ in the formula, bars of Type IV steel were assumed to be round and their effective diameters were determined from their cross-sectional areas. While the deformation of the bars used in this investigation had a pattern different from that used by Chi and Kirstein in their development of the expression for predicting the average crack width, no attempt was made to modify the coefficients in their formula to take into account the surface characteristics of the bars.

Comparison of the theoretical and observed crack widths in figure 21 indicates that the mean crack width was predicted with reasonable accuracy for bars of all six types. The shape of the stress-strain curve did not appear to have a consistent effect on the relationship between the mean crack width and the stress in the reinforcement.

The maximum values of steel stresses computed by both the "straight line" and the "ultimate strength design" 1/ theories are compared in Table 6 with the actual yield strengths obtained in tensile tests of the steel bars. The yield strengths given in the Table are the values obtained by the "halt of the gage" method for steels IA and II, while the values given for the other steels are based on an "offset" of 0.2 percent.

The agreement between the observed yield strengths and the maximum computed steel stresses was better for the straight line theory than for the ultimate strength design theory. Ratios of the maximum stresses computed by the straight line theory to the yield strengths ranged from 0.956 to 1.088, while for the ultimate strength design theory these ratios ranged from 1.057 to 1.180.

6. DISCUSSION OF RESULTS

This series of flexural beam tests was designed to study the effect of magnitude of steel stresses and the nature of the stress-strain characteristics on the performance of reinforced concrete beams.

It will be recalled that the beam specimens were designed so that the nominal total yield strength of the reinforcement ($f_y A_s$) was a constant. The control beams were designed to fail by yielding of the reinforcement and were reinforced with Type IA steel. Beams reinforced with 40,000 and 65,000 psi steel failed in tension, but beams with 100,000 psi reinforcement failed in compression or simultaneous compression and tension. All the beams failed at approximately equal loads.

The effect of the magnitude of steel stresses and the shape of the stress-strain curves on the center deflections, compressive strains in concrete and the average widths of cracks is shown in figures 8, 12, and 14 respectively. Attention is called to the fact that only in the case of the load-crack width relationship do the curves fall in three distinct groups corresponding to three nominal yield strengths of 40,000, 65,000 and 100,000 psi. In the case of deflections and particularly in the

---

1/ Ultimate strength design theory is that given in the Appendix of the ACI Building Code, ACI 318-56.

case of compressive strain in the concrete, the effect of the differences in the stress-strain characteristics and the corresponding differences in the moduli of steels became sufficiently pronounced to affect the relative standings of the several types of steel. This is brought out more clearly in figures 10, 13, and 15. As can be seen in figure 15, the effect of increasing the steel stress on the average width of cracks is essentially linear. Thus, at a given load causing stresses of 20,000, 32,500, and 50,000 psi in steels having nominal yield strengths of 40,000, 65,000, and 100,000 psi, respectively, the observed increases in crack widths were approximately 60 and 160 percent, or nearly the same as the increases in stress. The same relationship between increases in steel stresses and crack widths was observed for stresses ranging up to 90 percent of the nominal yield strengths of the steels. However, the relationship between the increases in the steel stresses and the observed increases in compressive strains, as well as in center deflections, is roughly linear only when the comparison is confined to the four steels having fairly linear stress-strain characteristics (steels IA, II, III and VA). For steels IV and VI, the effect of the curvilinear stress-strain characteristic on the deflections and compressive strain in the concrete can be clearly seen in figures 10 and 13. The effect of the lower modulus of steel on the increases in concrete strains is particularly pronounced for the twisted bar of Type IV steel. Reference to figure 2 indicates that the modulus of elasticity of steel bars of Type IV is 12 percent less than that of a conventional bar at a stress of 30,000 psi, while at a stress of 60,000 psi this difference increases to 28 percent. Similarly, for steel bars of Type VI, the modulus at stresses of 50,000 and 95,000 psi is about 13 percent and 27 percent less than that of a bar with a well defined yield strength.

Comparison between the observed values of steel stress and those computed by the straight line theory is indicated in figure 19. The agreement between the computed and observed stresses was closest for Type I steel. The difference between the computed and observed values became larger as the ratio of reinforcement and diameter of bars decreased.

Comparison of computed and observed values of deflections and compressive strains in the concrete is shown in figures 18 and 20. The deflections can be fairly accurately predicted provided the stress-strain characteristic of the steel does not depart significantly from a straight line and the crack pattern of the beam is substantially uniform along the entire span length, as shown in figures 6 and 7. The observed

deflections depart considerably from the computed values for steels exhibiting curvilinear stress-strain curves and gradual yielding, as in case of steels IV and VI. The comparison of observed compressive strains in concrete with the theoretical values shown in figure 20 indicates that the limitation of the "straight line theory" is more severe with respect to calculation of compressive stress than with respect to deflections. The departure of the observed compressive strains from the computed values becomes quite pronounced at higher loads, particularly for steels exhibiting gradual yielding.

The observed mean crack widths were compared with the theoretical values computed by means of Chi-Kirstein formula [3]. Comparison of the theoretical and observed crack widths shown in figure 21 indicates that the mean width of crack can be predicted with reasonable accuracy for all the steels used in this study. The shape of the stress-strain curve did not appear to have a consistent effect on the relationship between the crack width and the stress in the reinforcement.

The agreement between the computed maximum steel stresses and the observed yield strengths of the steels was better for the "straight line" theory than for the "ultimate load design" theory. Thus, the ratios of the maximum loads predicted by straight line theory to the observed loads ranged from 0.956 to 1.088, while for the ultimate load design theory these ratios ranged from 1.057 to 1.180. In general, the agreement between the computed and observed maximum loads was best for the steels with the highest yield strengths irrespective of the stress-strain characteristic.

7. References

[1] Arthur P. Clark, "Cracking in Reinforced Concrete Flexural Members," American Concrete Institute Journal, April 1956, Proceedings of, Vol. 52, page 851.

[2] D. Watstein and R. G. Mathey, "Evaluation of Width of Cracks in Concrete at the Surface of Reinforcing Steel by Means of Tensile Bond Specimens," Proceedings, Symposium on Bond and Crack Formation in Reinforced Concrete, Stockholm, 1957, pp. 253-260.

[3] Michael Chi and Arthur F. Kirstein, "Flexural Cracks in Reinforced Concrete Beams." (Manuscript has been submitted to the American Concrete Institute).

Table 1. Description of Beam Specimens.

Beam designation	Pieces and bar No.	Observed yield strength of reinforcement f_y	Area of reinforcement A_s	Total yield strength of reinforcement $A_s f_y$	Maximum load on beam	Ratio of reinforcement p	Concrete cylinder strength f'_c	Minimum spacing of cracks	Mode of failure
		psi	$in.^2$	lb	lb		psi	in.	
F-IA-22	2-No.9	42,500	1.960	83,300	64,500	0.0255	3520	4.31	tension
F-IA-23	2-No.9	42,500	1.960	83,300	67,500	0.0255	3590	4.06	tension
F-II-7	2-No.7	69,000	1.182	81,600	65,200	0.0154	3460	4.14	tension
F-II-12	2-No.7	69,000	1.182	81,600	63,900	0.0154	4200	4.73	tension
F-III-8	2-No.7	68,800	1.194	82,100	65,100	0.0155	3310	4.07	tension
F-III-13	2-No.7	68,800	1.194	82,100	64,500	0.0155	4010	4.80	tension
F-IV-20	1-W8,1-W9	70,500	1.198	84,500	61,700	0.0156	3380	4.01	tension
F-IV-21	1-W8,1-W9	70,500	1.198	84,500	61,700	0.0156	3470	4.38	tension
F-VA-17	2-No.6	98,800	0.864	85,400	63,200	0.0112	3810	4.73	compression
F-VA-19	2-No.6	98,800	0.864	85,400	62,100	0.0112	3630	5.86	uncertain 1/
F-VI-9	2-No.6	104,300	0.866	90,300	65,700	0.0113	3730	4.80	uncertain 1/
F-VI-18	2-No.6	104,300	0.866	90,300	63,300	0.0113	3730	4.65	compression

1/ Tensile and compressive failures appeared to have occurred simultaneously.

Table 2. Properties of Reinforcing Steel.

Type of steel	Size of bar	Area	Yield strength	Tensile strength	Modulus of elasticity	Elongation in 8 in.	Deformations				
							Width of gap	Average spacing	Average height	Average projected length	Bearing area
		$in.^2$	psi	psi	10^6 psi	%	in.	in.	in.	in.	$in.^2/in.$
IA	No.9	0.980	42,500 [1]	78,000	28.5	16.9	0.088	0.472	0.067	3.14	0.446
II	No.7	0.591	69,000 [1]	107,100	28.8	16.0	0.066	0.376	0.056	2.06	0.307
III	No.7	0.597	68,800 [2]	78,400	29.7 [3]	17.2	0.166	0.341	0.056	2.11	0.346
IV	W8	0.525	69,500 [2]	83,600	25.7	11.5	0.067	0.254	0.042	2.82	0.464
IV	W9	0.673	71,200 [2]	86,100	25.4	10.0	0.088	0.283	0.048	3.26	0.554
VA	No.6	0.432	98,800 [2]	120,600	28.1	6.5	0.142	0.324	0.048	1.82	0.269
VI	No.6	0.433	104,300 [2]	111,500	28.3	6.9	0.160	0.321	0.050	1.82	0.284

1/ Halt of gage method.

2/ 0.2 percent offset method.

3/ This value is high compared to other size bars of Type III steel. Average E = 28.5 x 10^6 psi for Type III steel.

Table 3. Properties of Deformations on Reinforcing Bars

Type of steel	Size of bar	Cross section area	Deformations					
			Width of gap	Average spacing	Average height	Height to diameter ratio	Average projected length	Bearing area
		$in.^2$	in.	in.	in.		in.	$in.^2/in.$
IA	No.9	0.980	0.088	0.472	0.067	0.600	3.14	0.446
II	No.6	0.432	0.074	0.325	0.047	0.634	1.77	0.256
II	No.9	1.003	0.105	0.448	0.052	0.460	2.66	0.309
III	No.6	0.455	0.175	0.308	0.044	0.578	1.87	0.267
III	No.9	0.987	0.205	0.517	0.061	0.544	2.70	0.319
IV	W6	0.294	0.072	0.203	0.027	0.441 1/	2.08	0.277
IV	W9	0.673	0.088	0.283	0.048	0.519 1/	3.27	0.554
VA	No.6	0.432	0.142	0.324	0.048	0.647	1.82	0.270
VA	No.9	0.977	0.180	0.514	0.061	0.547	2.70	0.320
VI	No.6	0.433	0.160	0.321	0.050	0.673	1.82	0.283
VI	No.9	0.986	0.207	0.512	0.060	0.535	2.77	0.325

1/ Bars of Type IV steel were assumed to be round and their effective diameters were determined from their cross-sectional areas.

Table 4. Grading of Aggregates
(White Marsh sand and gravel)

Sieve size	Cumulative Percent Retained	
	Sand	Gravel
1"	0.0	0.0
3/4"	0.0	27.00
1/2"	0.0	62.50
3/8"	0.0	83.10
1/4"	0.0	100.0
No. 4	1.98	
8	17.53	
16	31.49	
30	49.19	
50	76.55	
100	93.96	
Fineness Modulus	2.71	

Table 5. Values of Ø

Beam	Pieces and Bar No.	Ø
F-IA-22	2 - No. 9	0.757
F-IA-23	2 - No. 9	0.757
F-II-7	2 - No. 7	1.012
F-II-12	2 - No. 7	1.012
F-III-8	2 - No. 7	1.012
F-III-13	2 - No. 7	1.012
F-IV-20	1-W8, 1-W9	0.895
F-IV-21	1-W8, 1-W9	0.895
F-VA-17	2 - No. 6	0.964
F-VA-19	2 - No. 6	0.964
F-VI-9	2 - No. 6	0.964
F-VI-18	2 - No. 6	0.964

Table 6. Comparison of Computed Maximum Steel Stresses With Observed Yield Strengths.

Type of steel	Observed yield strength f_y	Straight line theory		Ultimate load design theory	
		Maximum steel stress f'_s	$\frac{f'_s}{f_y}$	Maximum steel stress f''_s	$\frac{f''_s}{f_y}$
	psi	psi		psi	
I	42,500	46,200	1.088	50,200	1.180
II	69,000	72,800	1.055	78,900	1.143
III	68,800	73,000	1.062	79,800	1.160
IV	70,500	68,800	0.975	75,700	1.074
VA	98,800	94,500	0.957	104,500	1.057
VI	104,300	99,700	0.956	110,500	1.060

Note: Yield strengths of steels IA and II were determined by "halt of gage" method; "offset" method was used for the other steels, with offset of 0.2 percent. Only those beams containing steels VA and VI (F-VA-19 and F-VI-9) which appeared to fail in tension were included in the above tabulation. For all other types of steel, the results of duplicate beam specimens are presented.

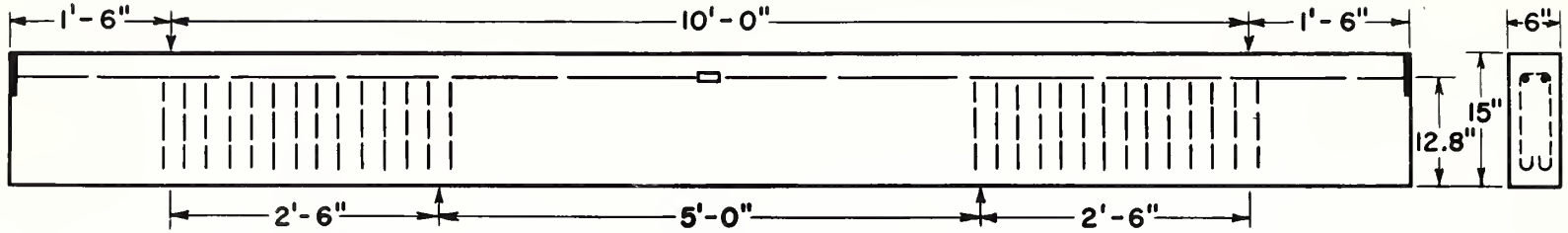

DIMENSIONS OF BEAM AND TYPE OF LOADING. STIRRUPS NO.3 BARS AT 2 $\frac{1}{2}$" SPACING

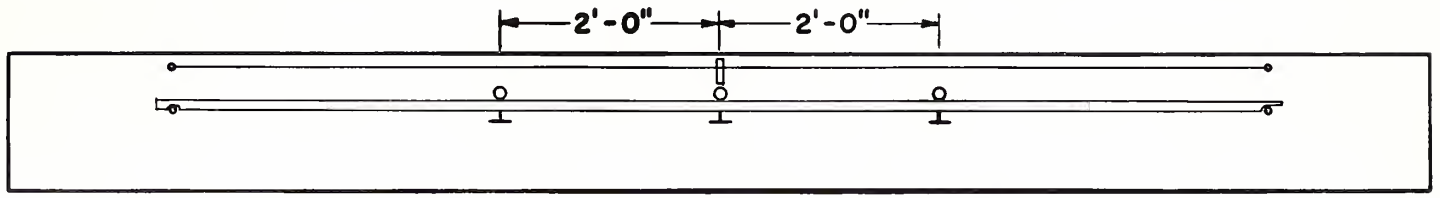

LOCATION OF DIAL GAGES AND TAUT WIRE FOR DEFLECTION MEASUREMENTS

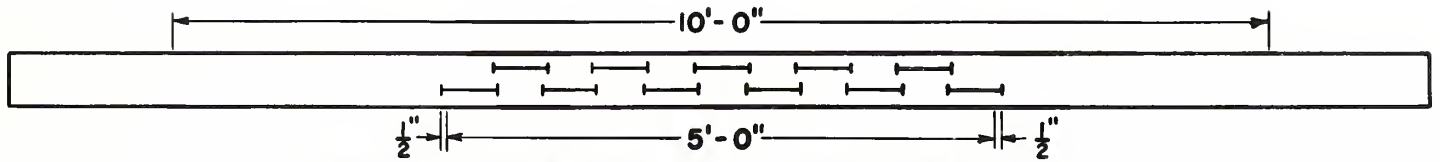

LOCATION OF TUCKERMAN STRAIN GAGES FOR MEASUREMENT OF WIDTH OF CRACKS

LOCATION OF BONDED WIRE STRAIN GAGES FOR MEASUREMENT OF COMPRESSIVE STRAINS

FIGURE 1. DESCRIPTION OF FLEXURAL TEST SPECIMEN AND INSTRUMENTATION.

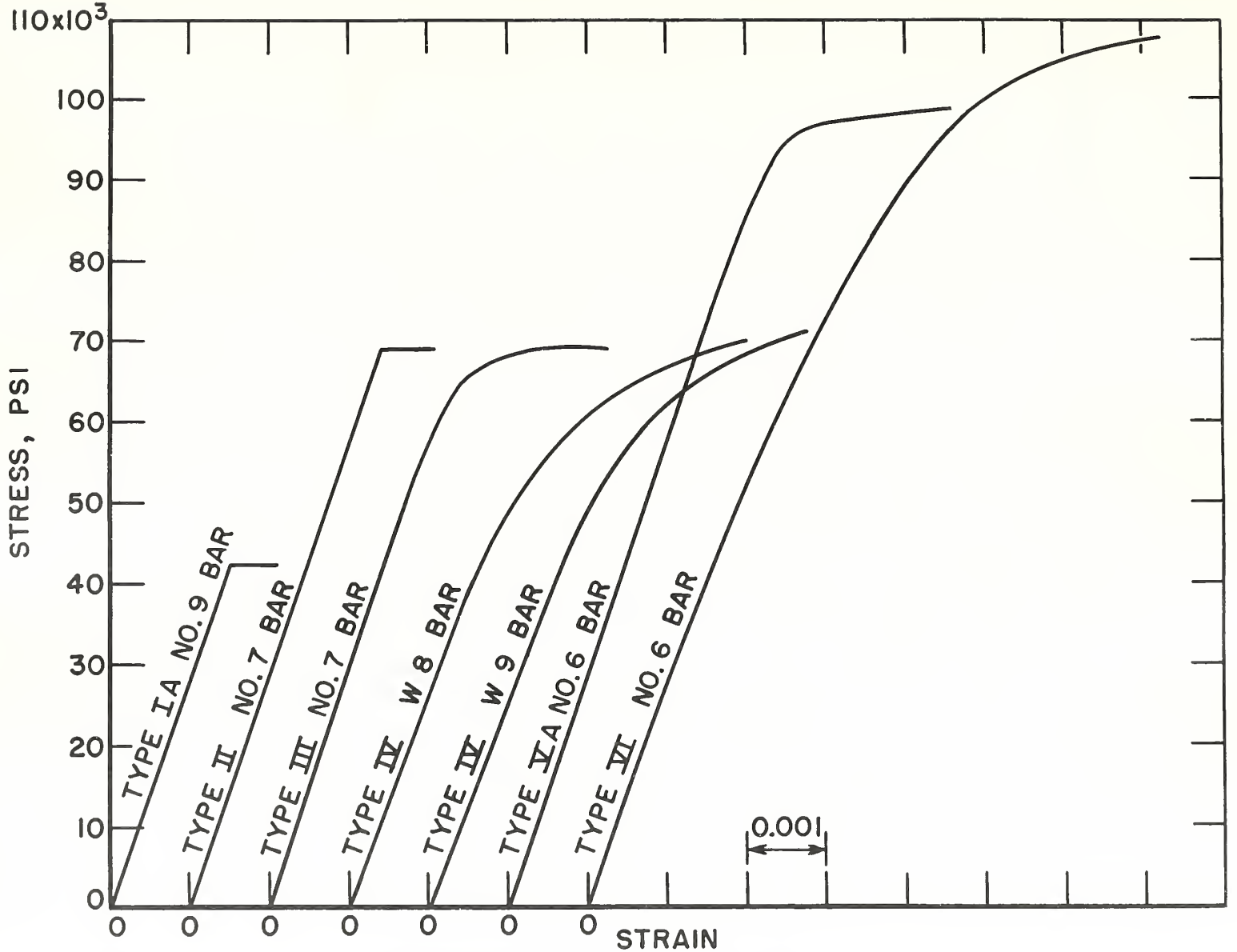

FIGURE 2. STRESS - STRAIN CHARACTERISTICS OF REINFORCING BARS.

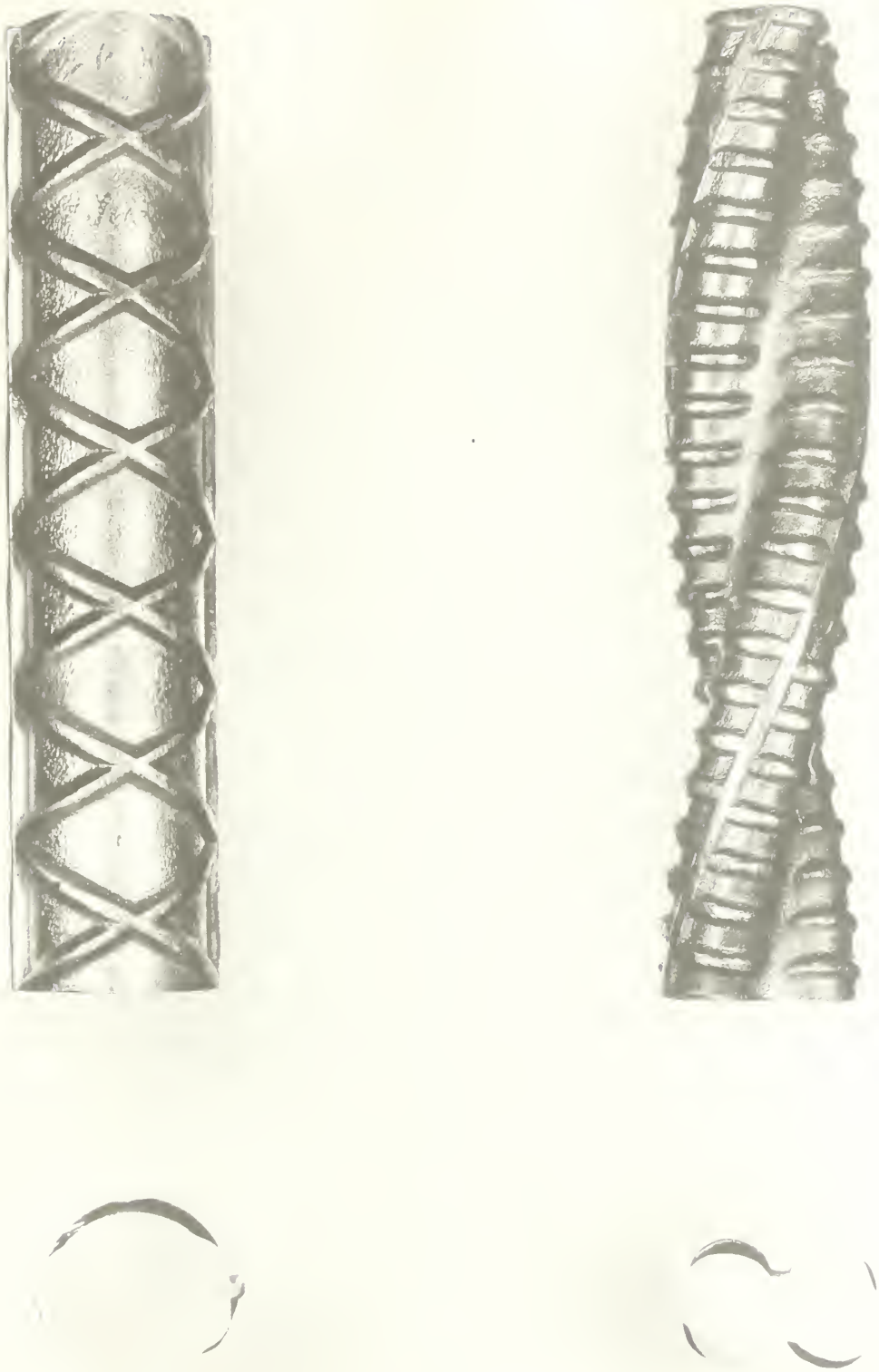

FIGURE 3. TYPICAL REINFORCING BARS USED IN BEAMS.

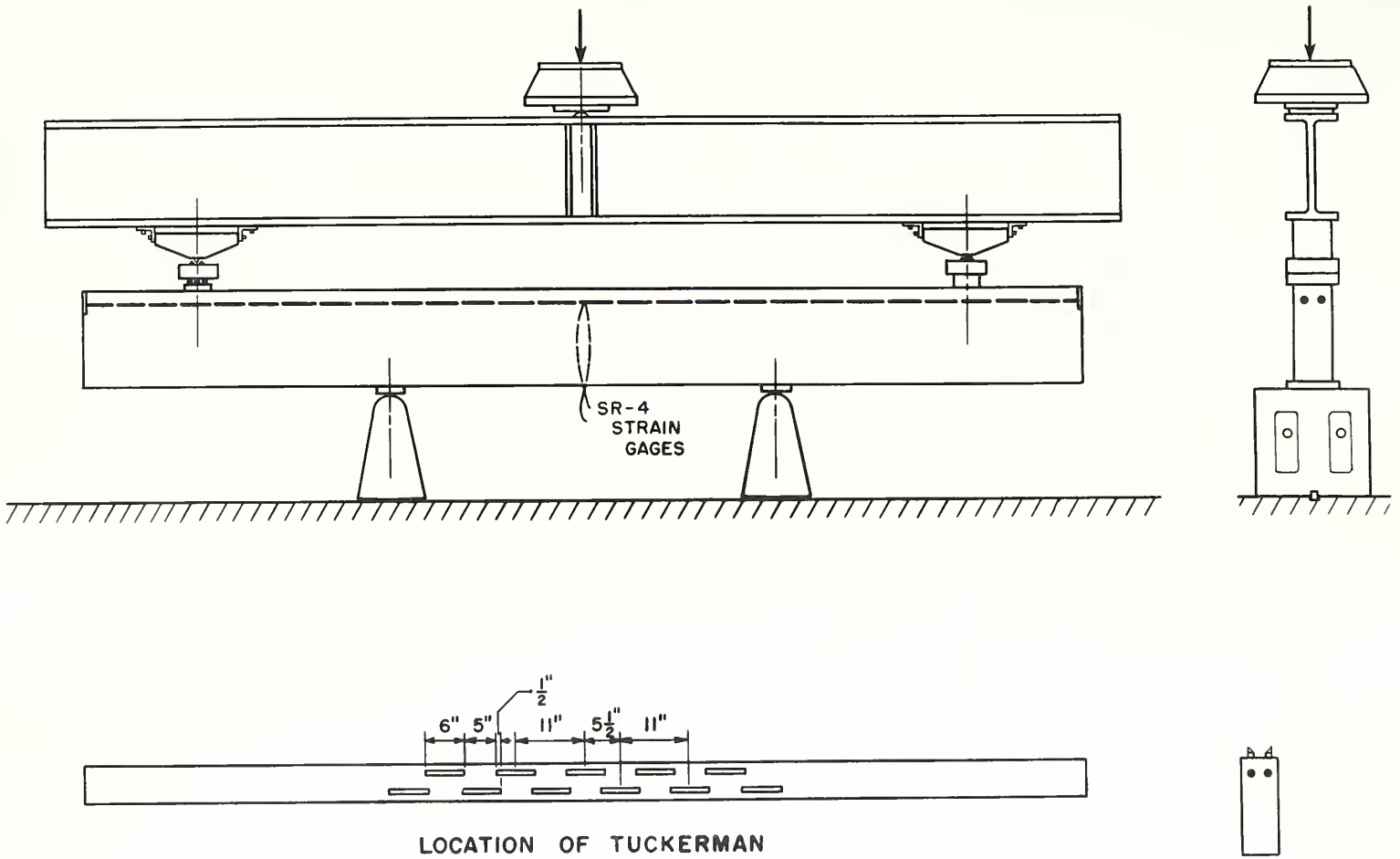

FIGURE 4. METHOD OF LOADING BEAM SPECIMEN AND ARRANGEMENT OF TUCKERMAN GAGES FOR MEASUREMENT OF WIDTH OF CRACKS.

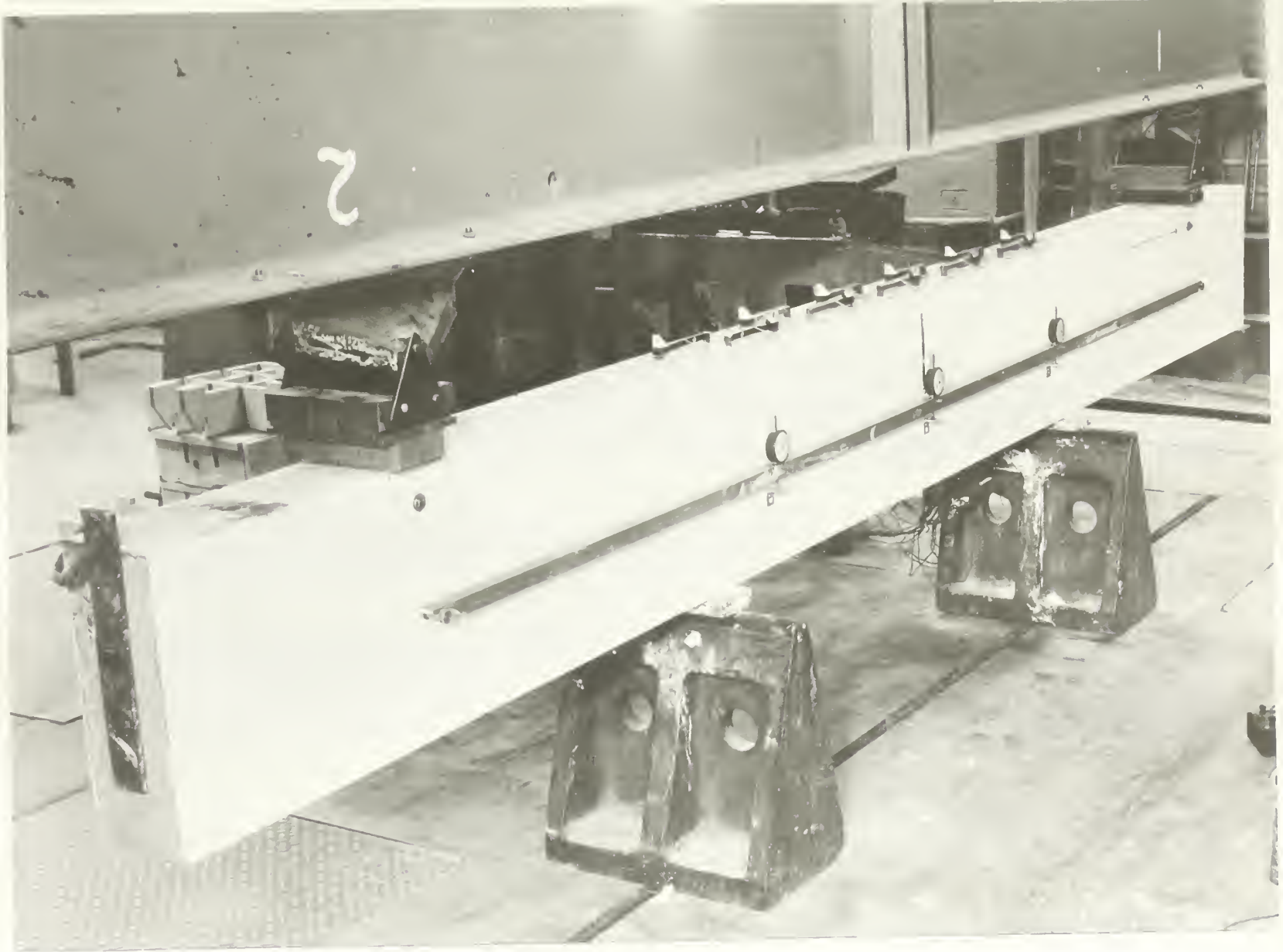

FIGURE 5. BEAM IN THE TESTING MACHINE PRIOR TO TESTING.

FIGURE 6. VIEWS OF BEAMS AFTER FAILURE.

FIGURE 7. VIEWS OF BEAMS AFTER FAILURE.

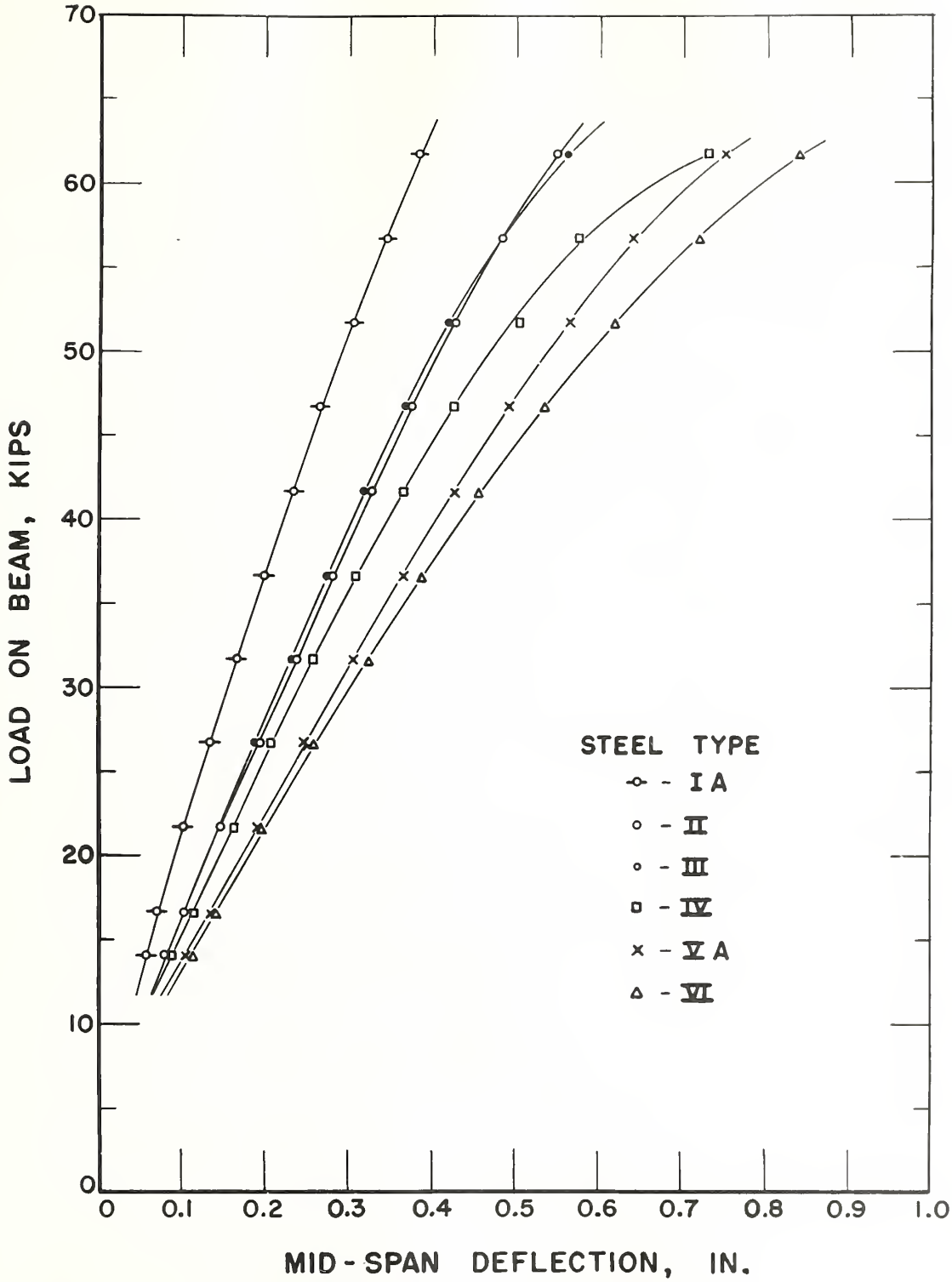

FIGURE 8. LOAD VS. MID-SPAN DEFLECTION.

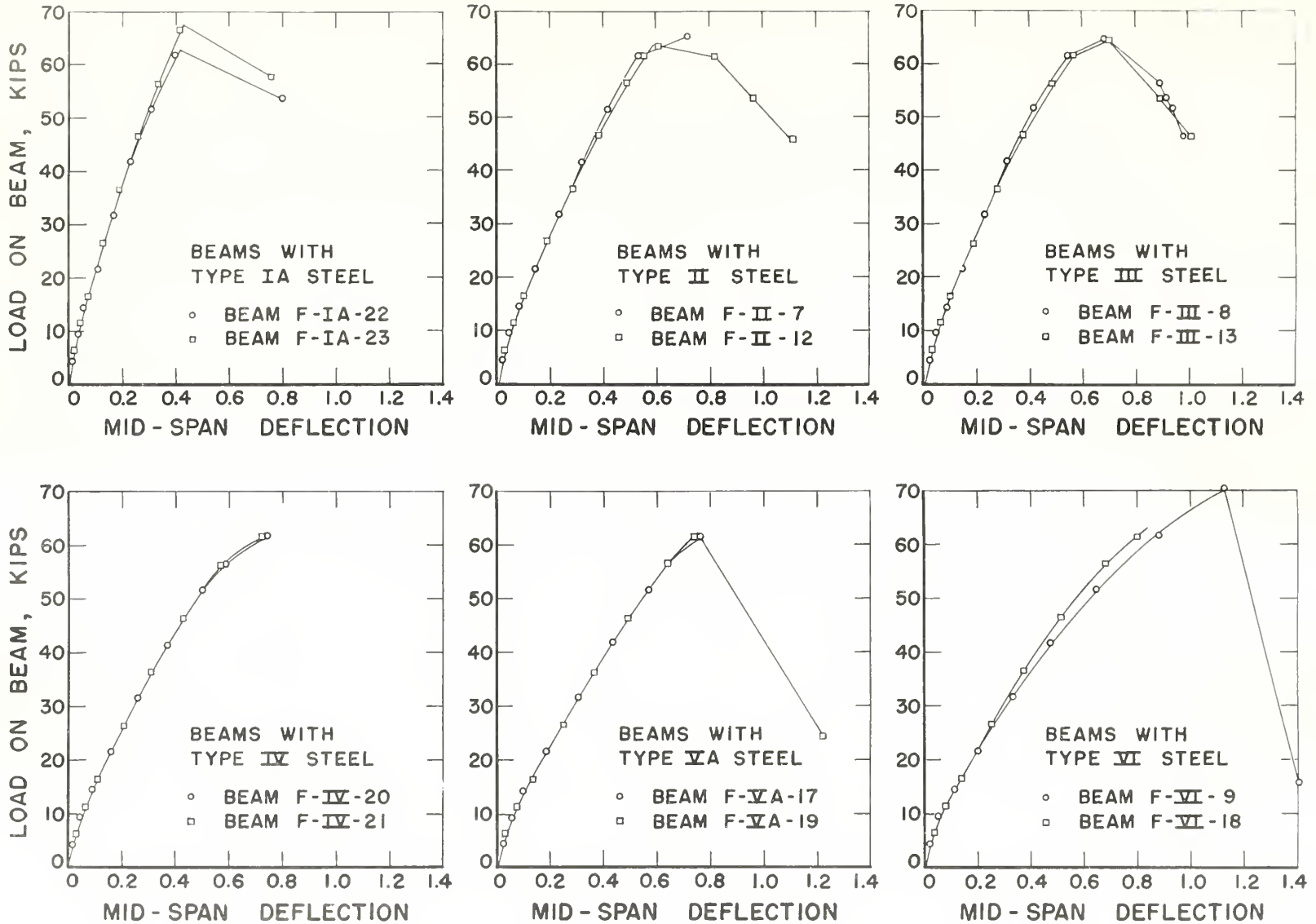

FIGURE 9. LOAD VS. MID-SPAN DEFLECTION TO POINT OF FAILURE.

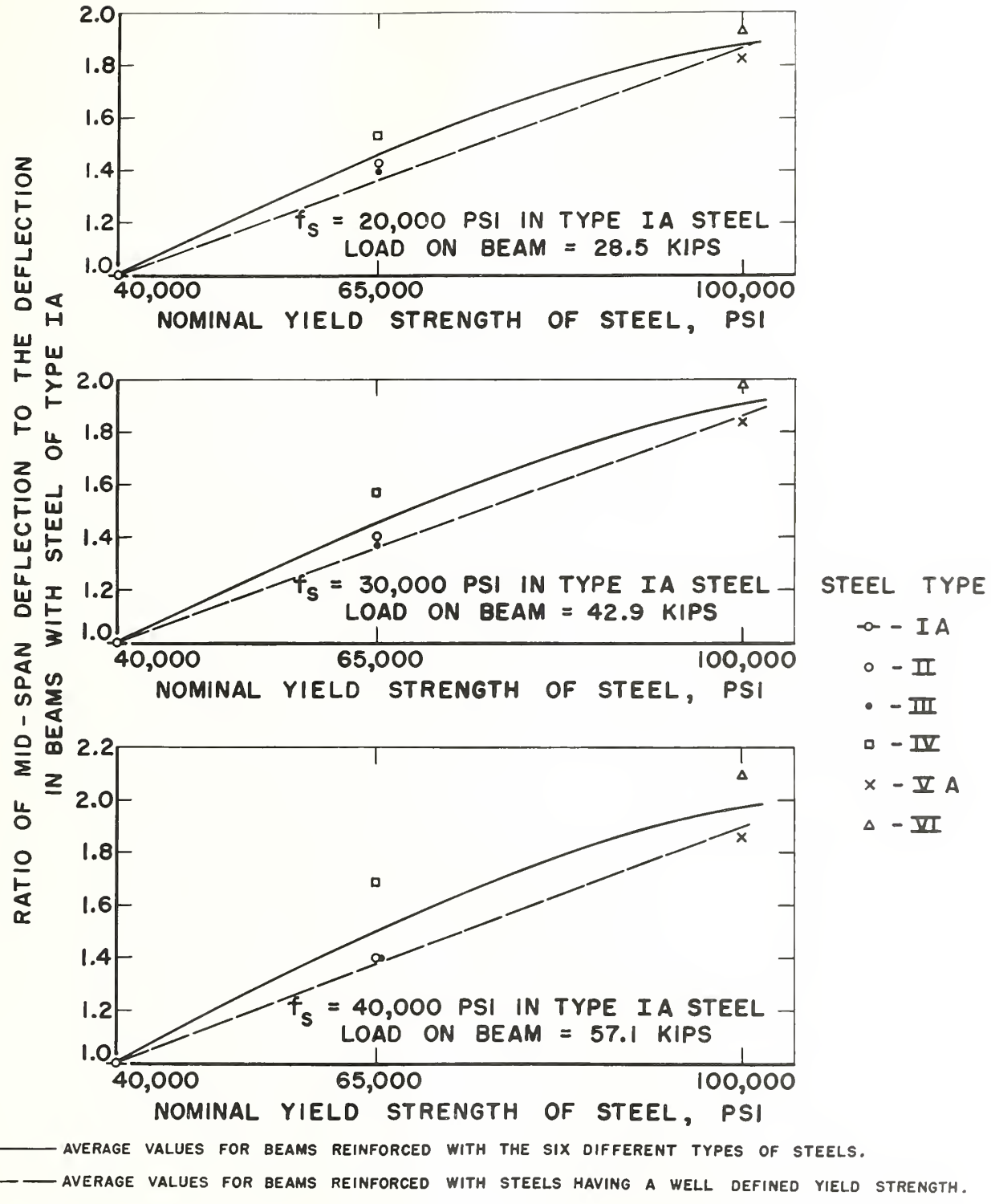

FIGURE 10. COMPARISON OF MID-SPAN DEFLECTION IN BEAMS SUPPORTING EQUAL LOADS.

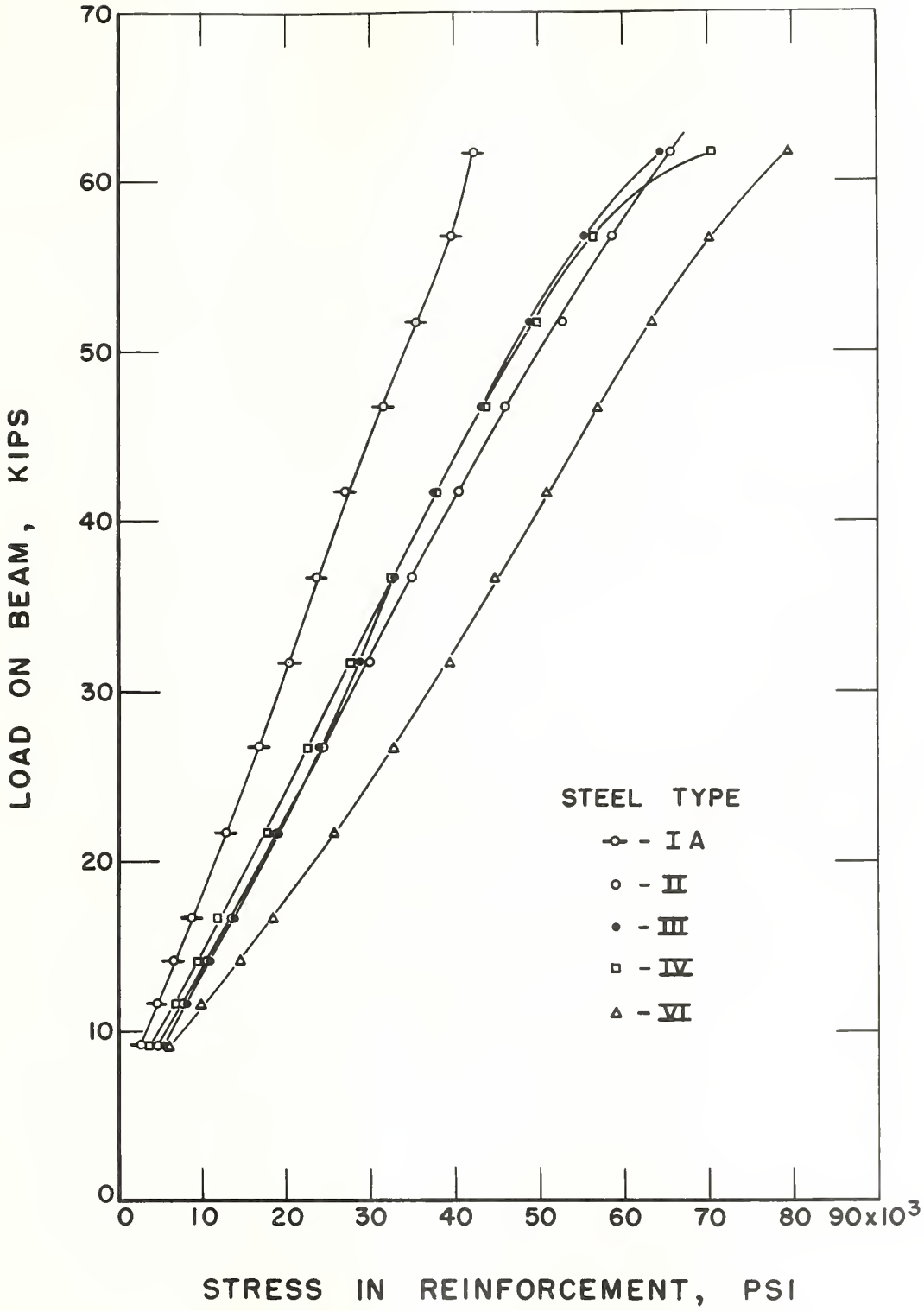

FIGURE 11. LOAD VS. OBSERVED STRESS IN REINFORCEMENT.

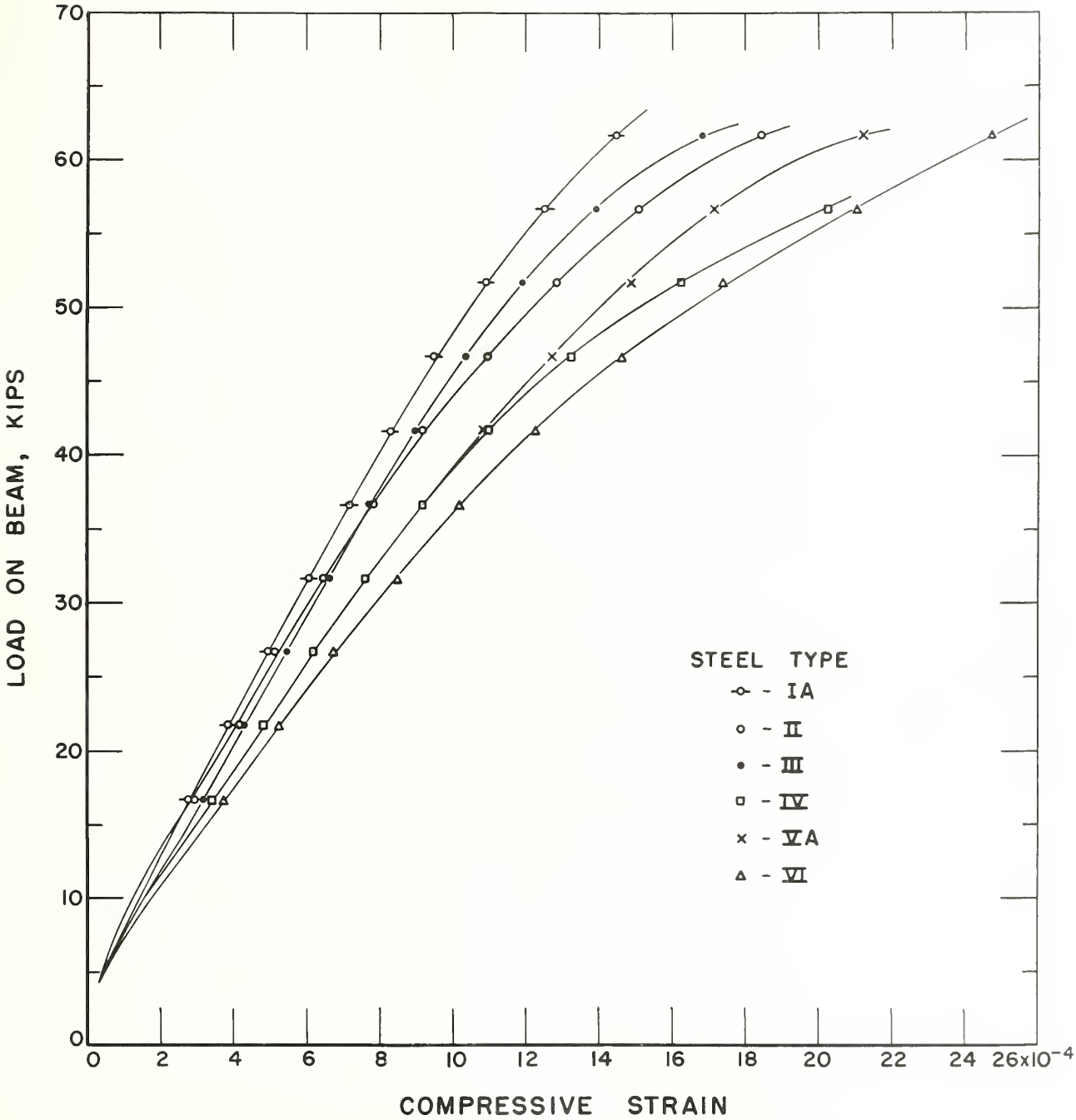

FIGURE 12. LOAD VS. COMPRESSIVE STRAIN IN CONCRETE.

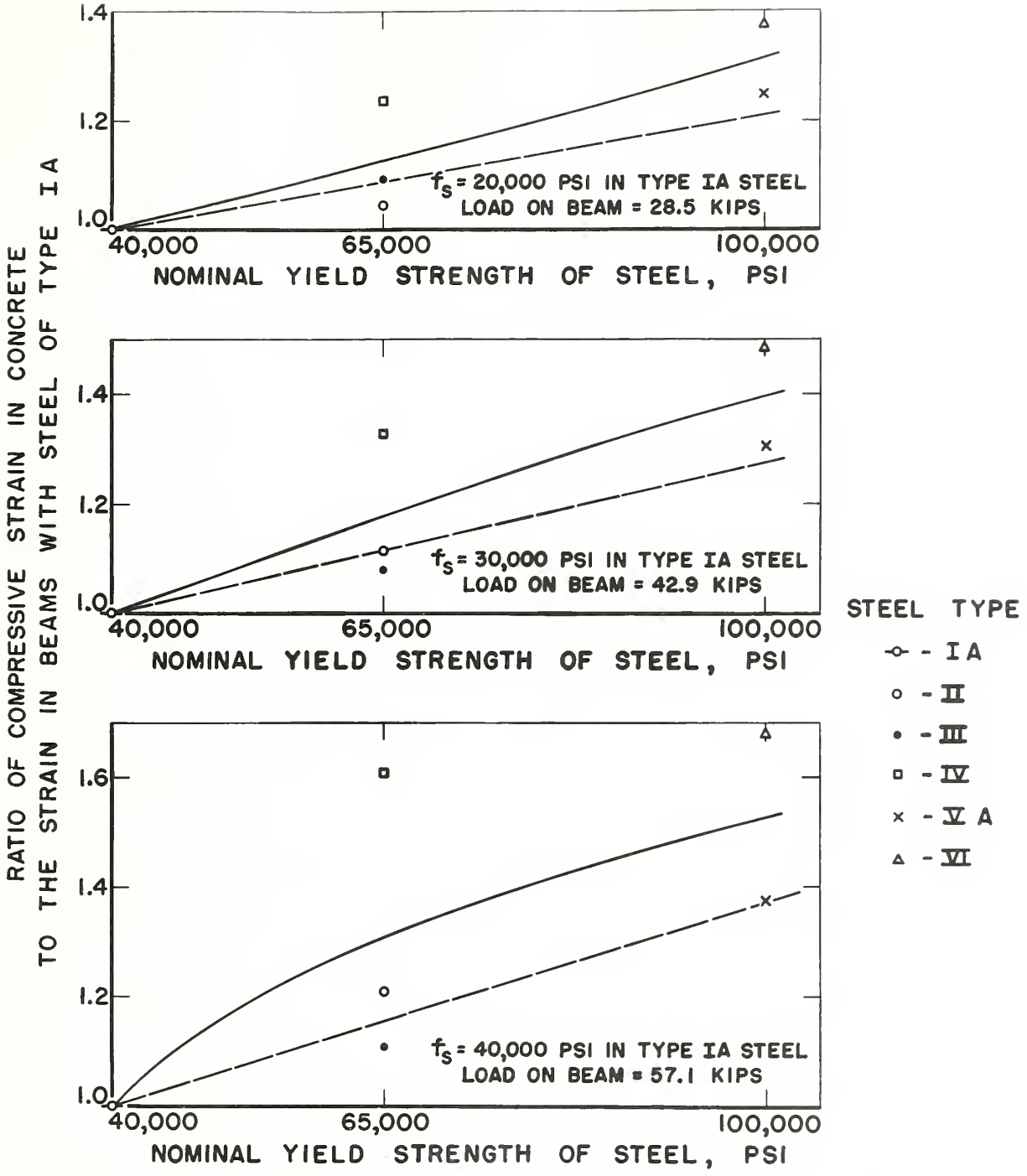

FIGURE 13. COMPARISON OF COMPRESSIVE STRAINS IN BEAMS SUPPORTING EQUAL LOADS.

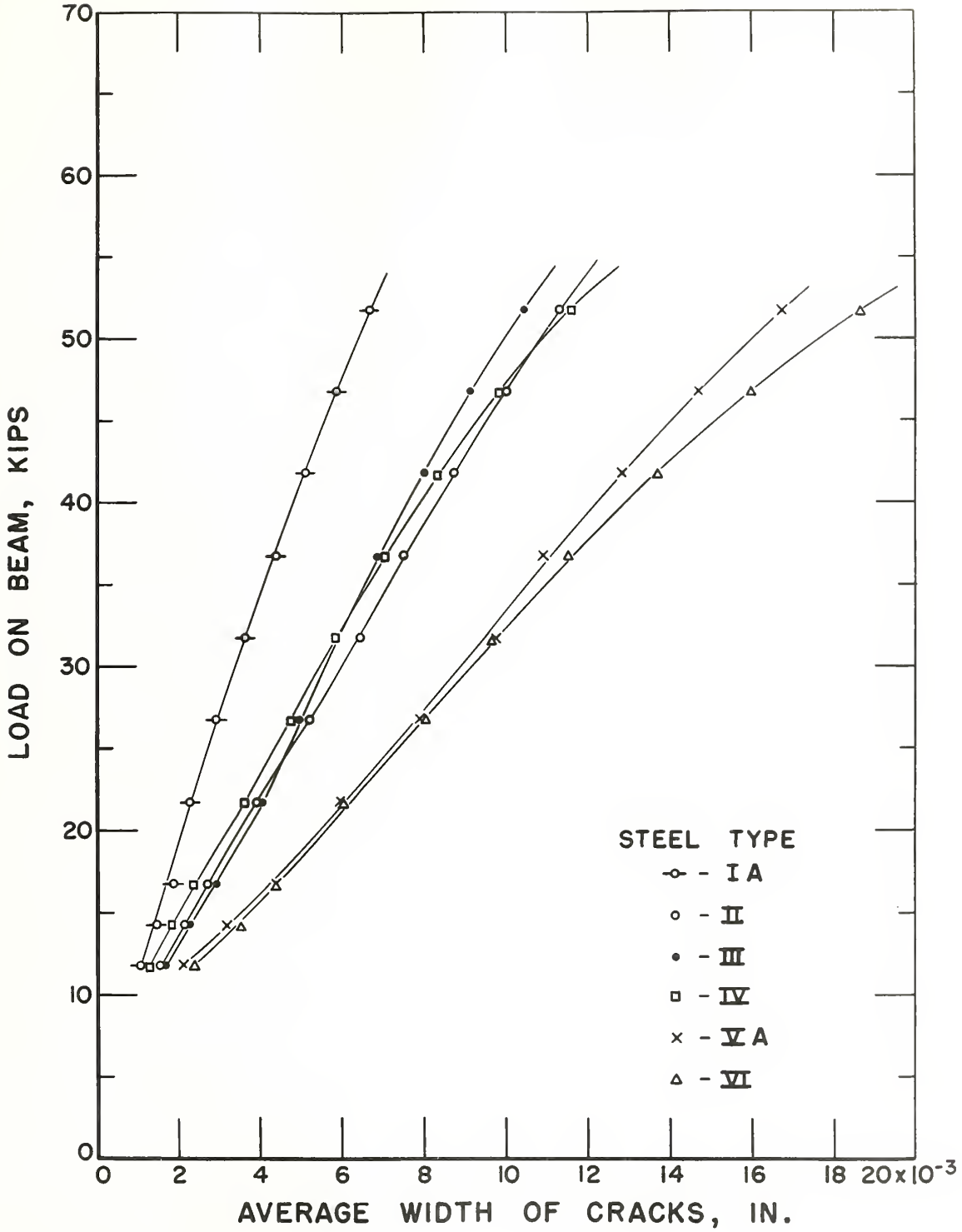

FIGURE 14. LOAD VS. AVERAGE WIDTH OF CRACKS.

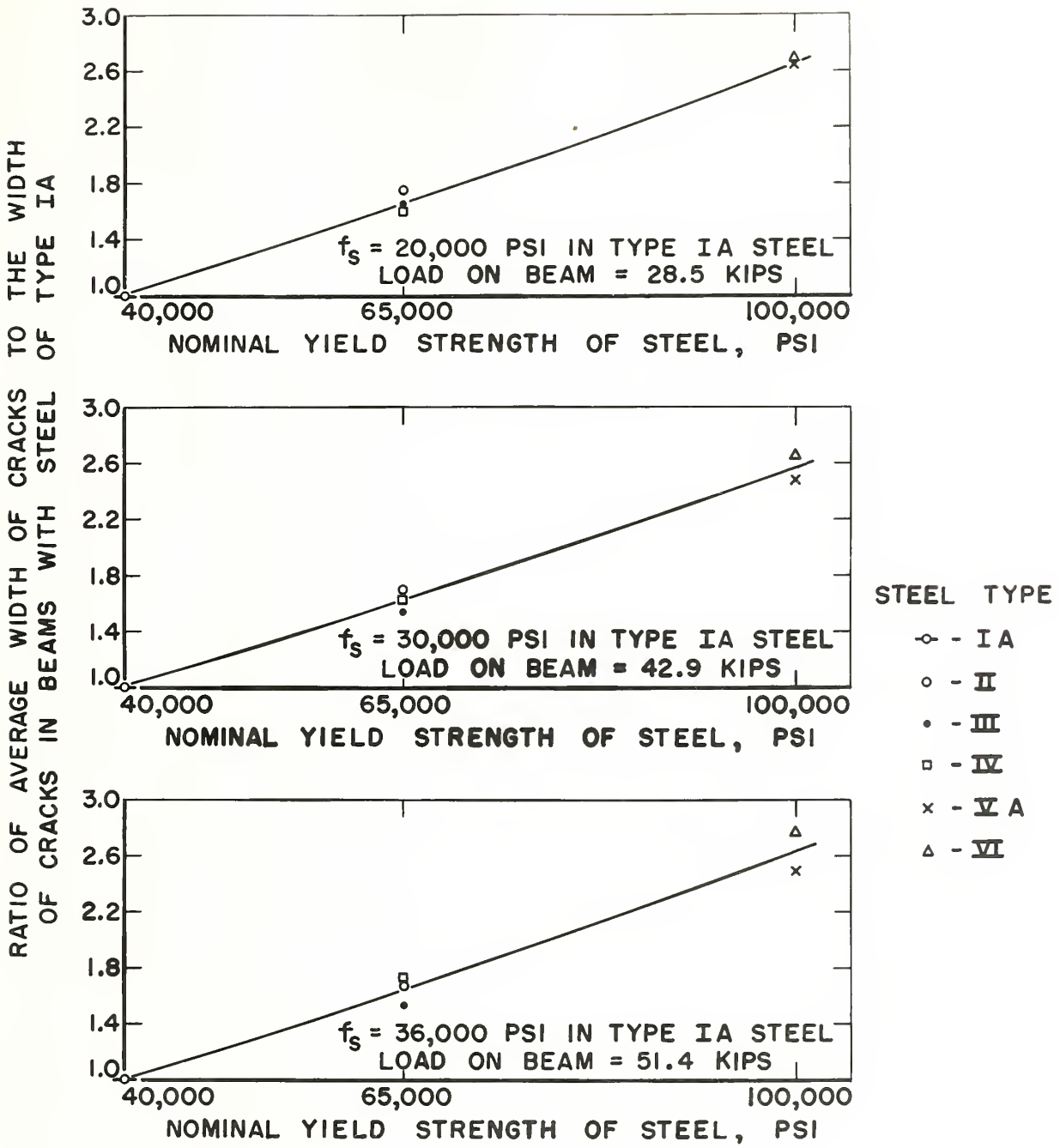

FIGURE 15. COMPARISON OF AVERAGE WIDTH OF CRACKS IN BEAMS SUPPORTING EQUAL LOADS.

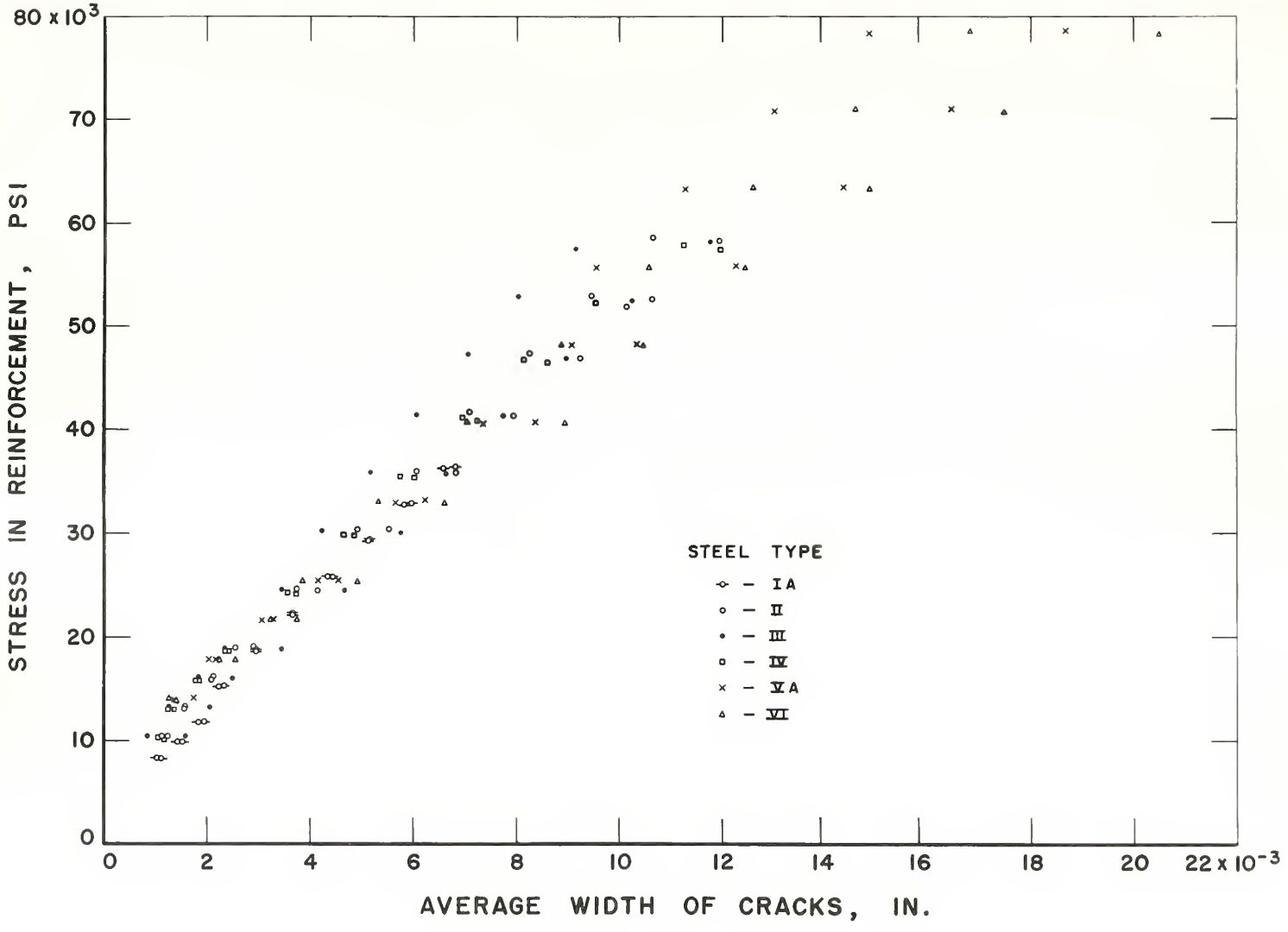

FIGURE 16. THEORETICAL STRESS IN THE REINFORCEMENT VS. AVERAGE WIDTH OF CRACKS.
(FOR INDIVIDUAL BEAM SPECIMENS)

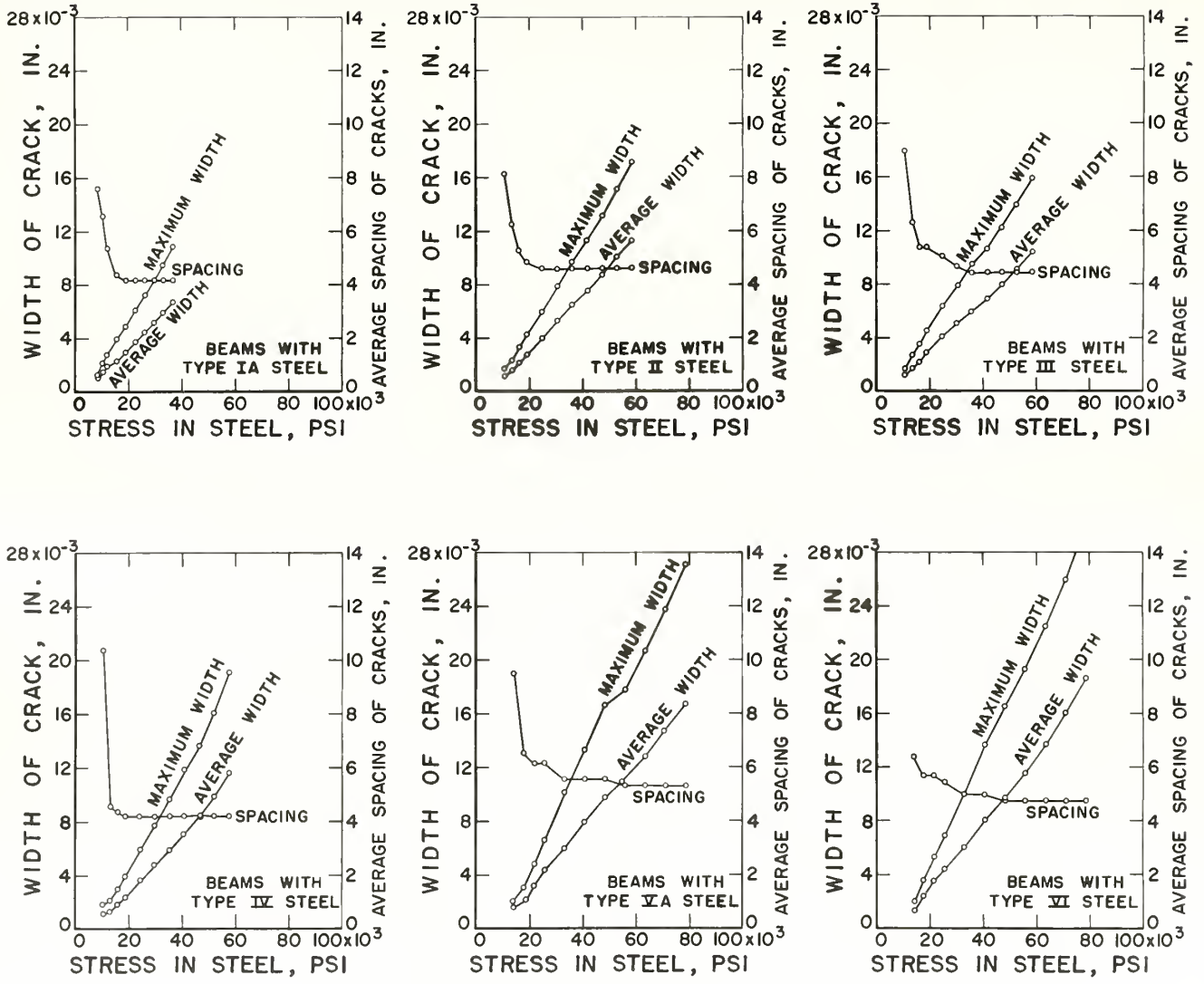

FIGURE 17. THEORETICAL STRESS IN THE REINFORCEMENT VS. SPACING, AND MAXIMUM AND AVERAGE WIDTH OF CRACKS.

(DATA AVERAGED FOR TWO BEAM SPECIMENS WITH EACH TYPE OF STEEL)

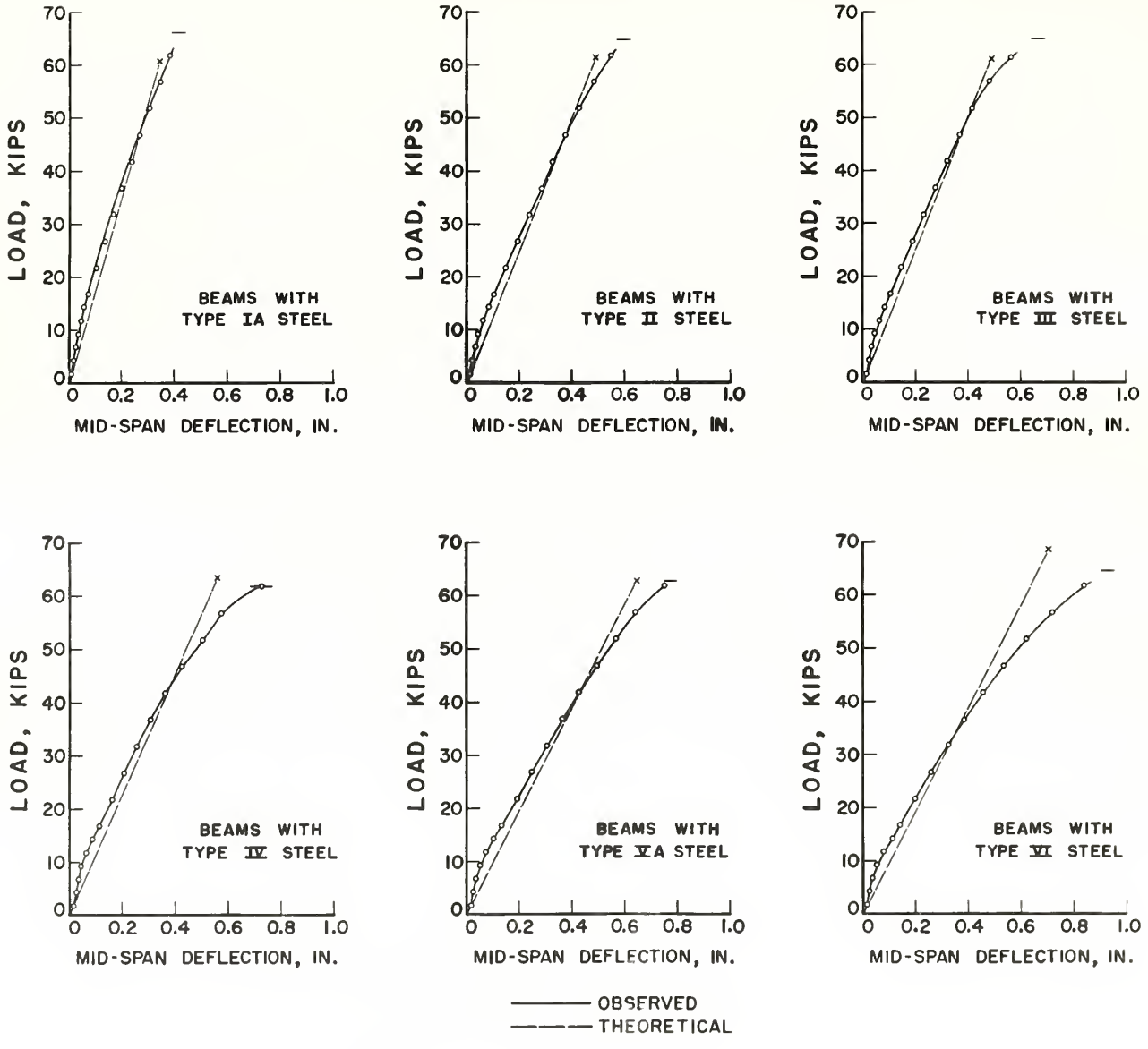

FIGURE 18. COMPARISON OF THEORETICAL AND OBSERVED MID-SPAN DEFLECTIONS.

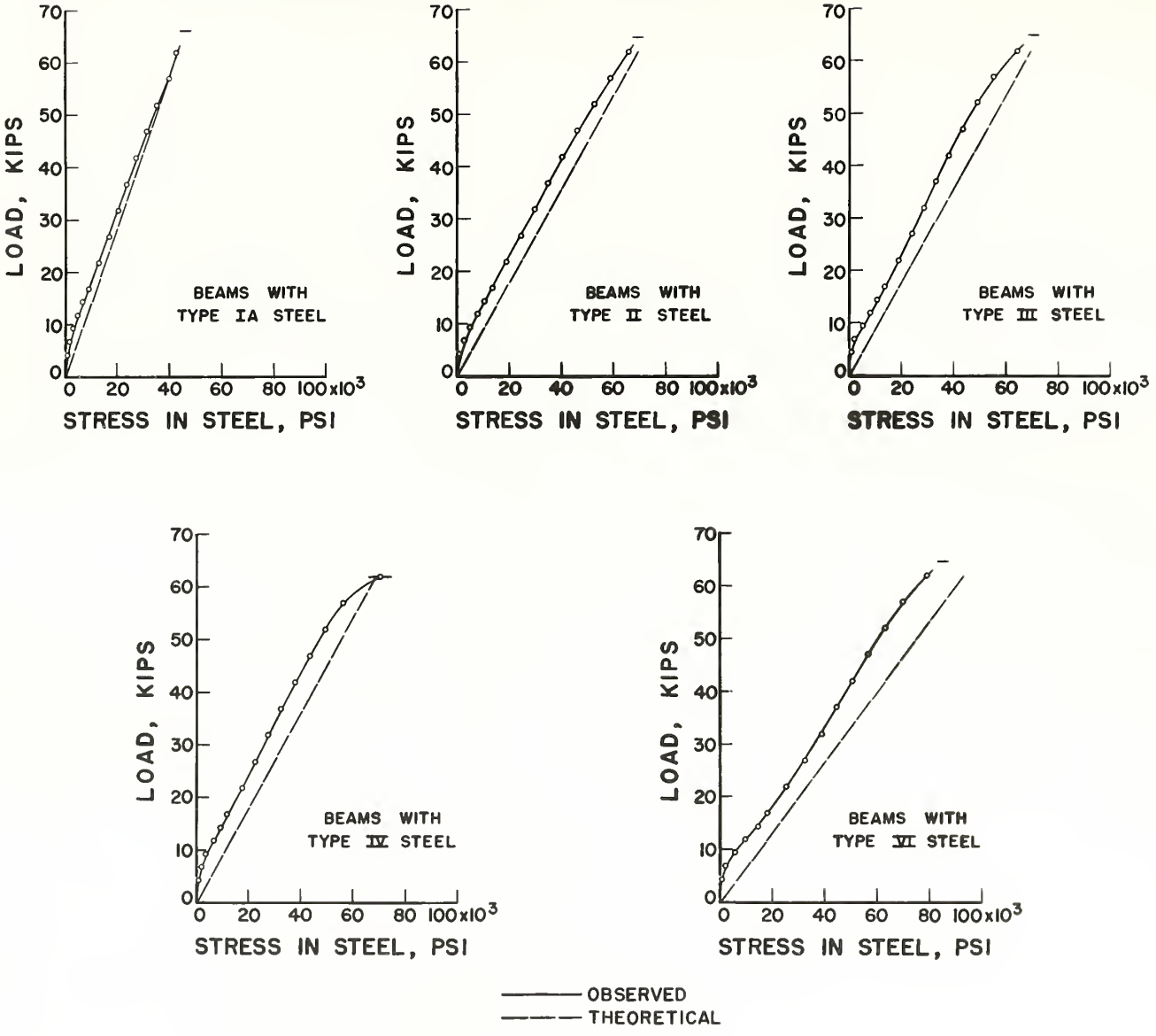

FIGURE 19. COMPARISON OF THEORETICAL AND OBSERVED STRESSES IN THE REINFORCEMENT.

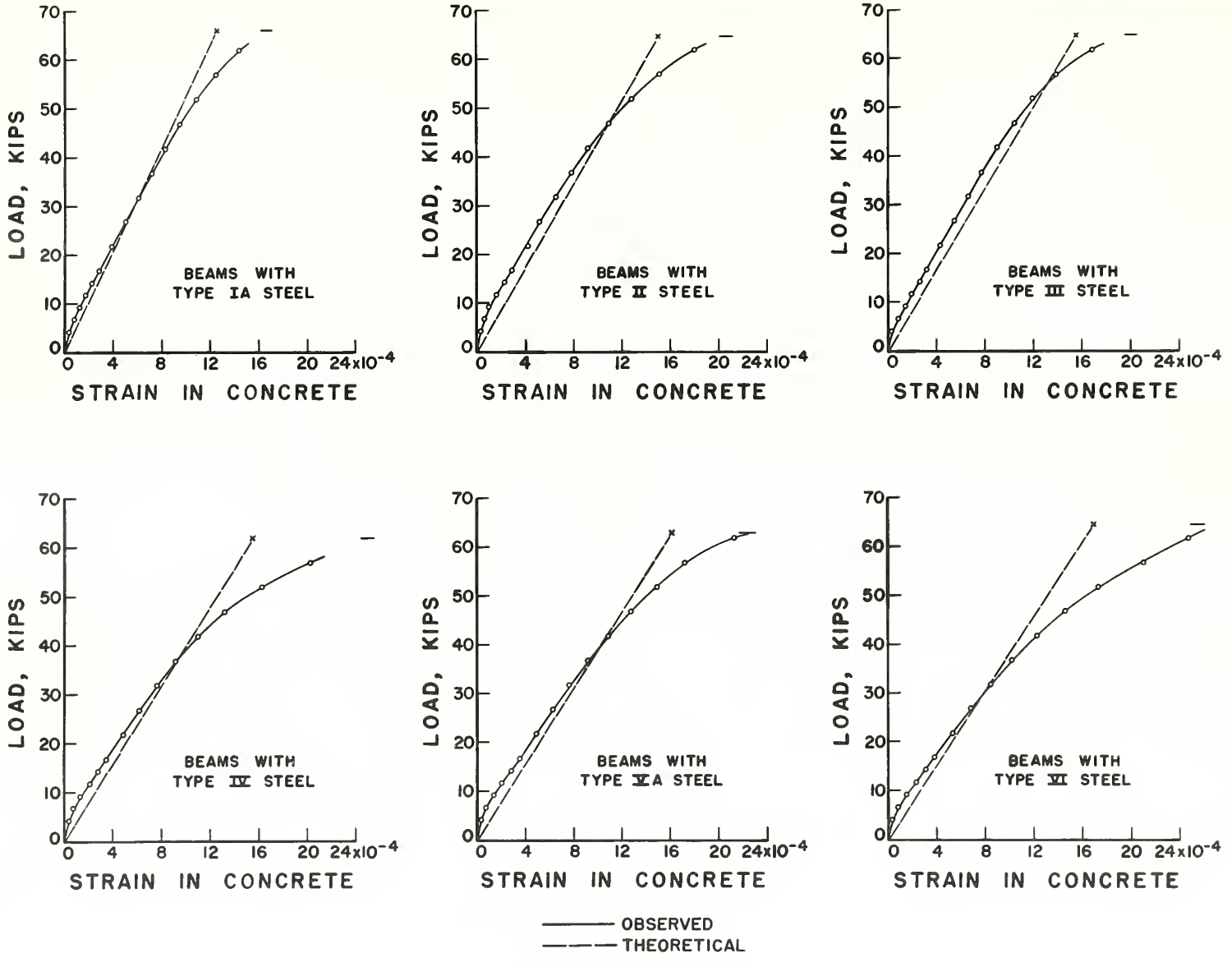

FIGURE 20. COMPARISON OF THEORETICAL AND OBSERVED CONCRETE STRAINS.

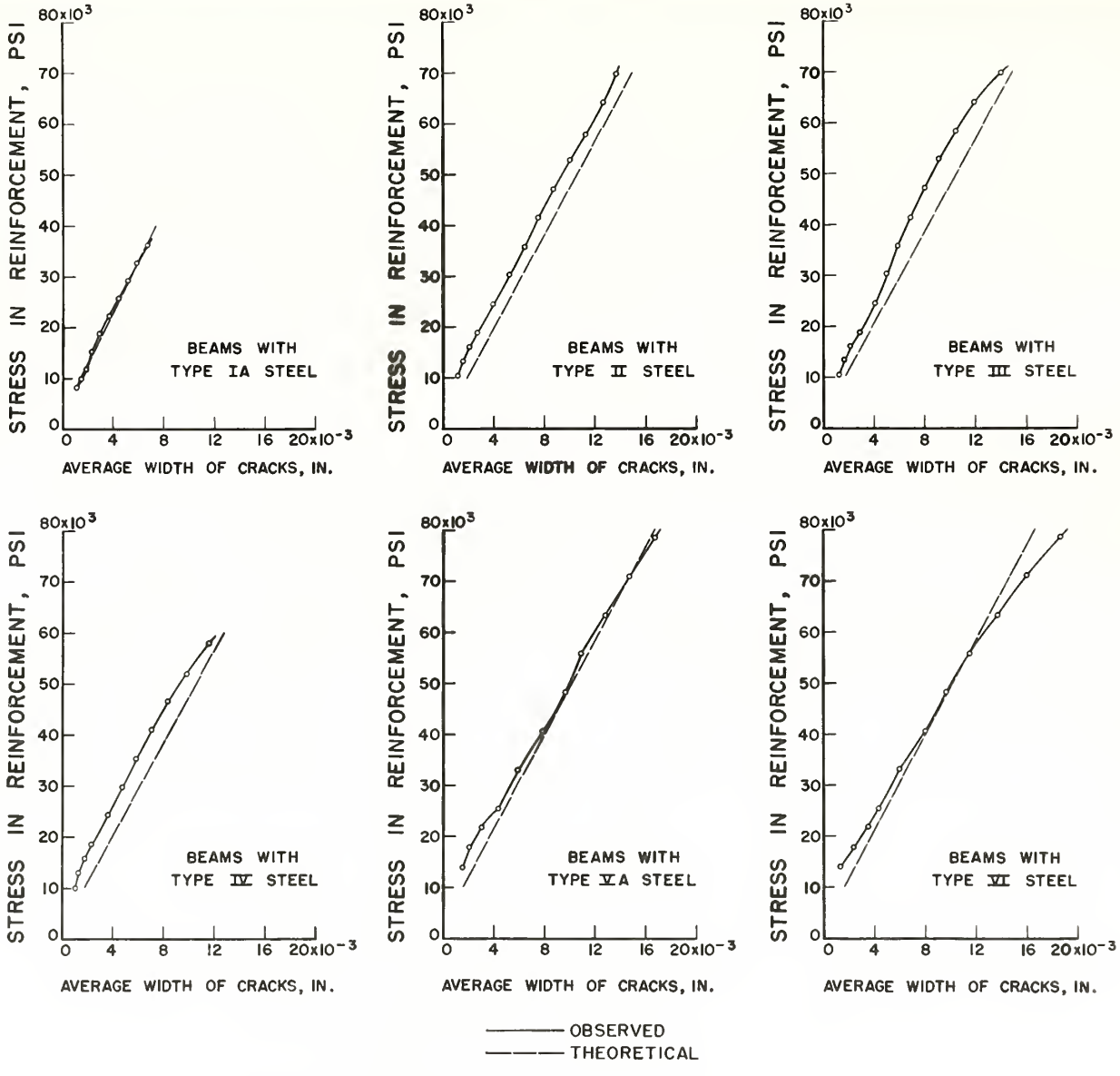

FIGURE 21. COMPARISON OF THEORETICAL AND OBSERVED WIDTH OF CRACKS.

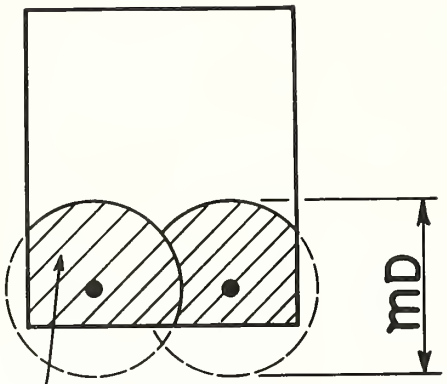

A_t = ASSUMED EFFECTIVE AREA

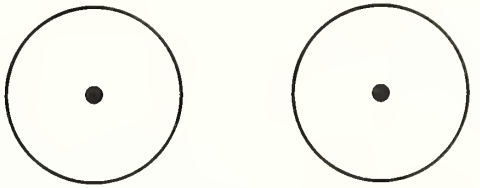

FULLY DEVELOPED AREA = $m^2 A_s$

$$\phi = \frac{A_t}{m^2 A_s}$$

FIGURE 22. CROSS SECTION OF BEAM ILLUSTRATING THE PARAMETER ϕ.

U. S. DEPARTMENT OF COMMERCE
Sinclair Weeks, *Secretary*

NATIONAL BUREAU OF STANDARDS
A. V. Astin, *Director*

THE NATIONAL BUREAU OF STANDARDS

The scope of activities of the National Bureau of Standards at its headquarters in Washington, D. C., and its major field laboratories in Boulder, Colorado, is suggested in the following listing of the divisions and sections engaged in technical work. In general, each section carries out specialized research, development, and engineering in the field indicated by its title. A brief description of the activities, and of the resultant reports and publications, appears on the inside front cover of this report.

WASHINGTON, D. C.

Electricity and Electronics. Resistance and Reactance. Electron Tubes. Electrical Instruments. Magnetic Measurements. Dielectrics. Engineering Electronics. Electronic Instrumentation. Electrochemistry.

Optics and Metrology. Photometry and Colorimetry. Optical Instruments. Photographic Technology. Length. Engineering Metrology.

Heat and Power. Temperature Physics. Thermodynamics. Cryogenic Physics. Rheology and Lubrication. Engine Fuels.

Atomic and Radiation Physics. Spectroscopy. Radiometry. Mass Spectrometry. Solid State Physics. Electron Physics. Atomic Physics. Nuclear Physics. Radioactivity. X-rays. Betatron. Nucleonic Instrumentation. Radiological Equipment. AEC Radiation Instruments.

Chemistry. Organic Coatings. Surface Chemistry. Organic Chemistry. Analytical Chemistry. Inorganic Chemistry. Electrodeposition. Gas Chemistry. Physical Chemistry. Thermochemistry. Spectrochemistry. Pure Substances.

Mechanics. Sound. Mechanical Instruments. Fluid Mechanics. Engineering Mechanics. Mass and Scale. Capacity, Density, and Fluid Meters. Combustion Controls.

Organic and Fibrous Materials. Rubber. Textiles. Paper. Leather. Testing and Specifications. Polymer Structure. Organic Plastics. Dental Research.

Metallurgy. Thermal Metallurgy. Chemical Metallurgy. Mechanical Metallurgy. Corrosion. Metal Physics.

Mineral Products. Engineering Ceramics. Glass. Refractories. Enameled Metals. Concreting Materials. Constitution and Microstructure.

Building Technology. Structural Engineering. Fire Protection. Heating and Air Conditioning. Floor, Roof, and Wall Coverings. Codes and Specifications.

Applied Mathematics. Numerical Analysis. Computation. Statistical Engineering. Mathematical Physics.

Data Processing Systems. SEAC Engineering Group. Components and Techniques. Digital Circuitry. Digital Systems. Analogue Systems. Application Engineering.

• Office of Basic Instrumentation

• Office of Weights and Measures

BOULDER, COLORADO

Cryogenic Engineering. Cryogenic Equipment. Cryogenic Processes. Properties of Materials. Gas Liquefaction.

Radio Propagation Physics. Upper Atmosphere Research. Ionospheric Research. Regular Propagation Services. Sun-Earth Relationships.

Radio Propagation Engineering. Data Reduction Instrumentation. Modulation Systems. Navigation Systems. Radio Noise. Tropospheric Measurements. Tropospheric Analysis. Radio Systems Application Engineering.

Radio Standards. Radio Frequencies. Microwave Frequencies. High Frequency Electrical Standards. Radio Broadcast Service. High Frequency Impedance Standards. Calibration Center. Microwave Physics. Microwave Circuit Standards.


NBS